

Revisiting Lossless Convexification: Theoretical Guarantees for Discrete-time Optimal Control Problems

Dayou Luo ^a, Kazuya Echigo ^b, and Behçet Açıkmeşe ^b

^a*Department of Applied Mathematics, University of Washington, Seattle, WA, 98195*

^b*William E. Boeing Department of Aeronautics and Astronautics, University of Washington, Seattle, WA, 98195*

Abstract

Lossless Convexification (LCvx) is a modeling approach that transforms a class of nonconvex optimal control problems, where nonconvexity primarily arises from control constraints, into convex problems through convex relaxations. These convex problems can be solved using polynomial-time numerical methods after discretization, which converts the original infinite-dimensional problem into a finite-dimensional one. However, existing LCvx theory is limited to continuous-time optimal control problems, as the equivalence between the relaxed convex problem and the original nonconvex problem holds only in continuous-time. This paper extends LCvx theory to discrete-time optimal control problems by classifying them into normal and long-horizon cases. For normal cases, after an arbitrarily small perturbation to the system dynamics (recursive equality constraints), applying the existing LCvx method to discrete-time problems results in optimal controls that meet the original nonconvex constraints at all but no more than $n_x - 1$ temporal grid points, where n_x is the state dimension. For long-horizon cases, the existing LCvx method fails, but we resolve this issue by integrating it with a bisection search, leveraging the continuity of the value function from the relaxed convex problem to achieve similar results as in normal cases. This paper strengthens the theoretical foundation of LCvx, extending the applicability of LCvx theory to discrete-time optimal control problems.

1 Introduction

Lossless Convexification (LCvx) is a technique designed to efficiently solve a class of nonconvex continuous-time optimal control problems, where nonconvexity primarily arises from control constraints. The central idea of LCvx is to introduce slack variables to relax these nonconvex constraints, thereby converting the nonconvex feasible set into a convex one. Importantly, under mild conditions, Pontryagin’s maximum principle guarantees that the solution of this relaxed convex formulation remains feasible and optimal for the original nonconvex problem. As this relaxation introduces no approximation error or loss in solution quality, the technique is termed “lossless” [Açıkmeşe and Ploen, 2005]. Once reformulated, the continuous time problem can be discretized into a finite-dimensional convex optimization problem and efficiently solved using standard polynomial-time interior solvers Nemirovski [2004].

LCvx research has been active for the past decade, and it has proven useful in numerous applications [Malyuta et al., 2022]. The initial application of the LCvx method targeted Mars pinpoint landings [Açıkmeşe and Ploen, 2005, 2007], where the nonzero lower bound on the magnitude of the control input vector led to non-

convex control constraints. Later, the LCvx family has been generalized to handle a wide range of continuous-time optimal control problems, including but not limited to those with generalized nonconvex input constraints [Açıkmeşe and Blackmore, 2011, Yang and Liu, 2023], input pointing constraints [Carson et al., 2011], integer constraints [Harris, 2021, Woodford and Harris, 2021, Echigo et al., 2023, 2024, Malyuta and Açıkmeşe, 2020], active fault diagnosis [Guo et al., 2024], as well as problems with additional convex affine and quadratic state constraints [Harris and Açıkmeşe, 2013, 2014]. Moreover, the efficacy of the LCvx method has also been tested in real-world experiments [Açıkmeşe et al., 2012, 2013] and is now being used as a baseline for Moon landing applications [Fritz et al., 2022, Shaffer et al., 2024].

Despite the success of LCvx in real-world applications, its theoretical results do not fully support its practical use. While LCvx theory establishes an equivalence between a continuous-time nonconvex optimal control problem and its convex relaxation, both remain continuous-time problems and cannot be directly solved by numerical solvers, which handle only finite-dimensional problems. To address this, discretization is usually applied to transform both problems into finite-dimensional, discrete-time versions [Açıkmeşe and Blackmore, 2011]. However, this discretization

* Corresponding author Dayou Luo.

step introduces additional theoretical challenges, as continuous-time LCvx theory does not guarantee that the optimal solution of the discretized convex relaxation satisfies the constraints of the discretized nonconvex problem, and thus it does not guarantee the equivalence between these two discrete problems.

In fact, the optimal solution of the discrete-time convex relaxation can violate the constraints of the original discrete-time nonconvex problem, a phenomenon previously observed in LCvx research [Açikmeşe and Ploen, 2007, Malyuta and Açikmeşe, 2020]. In this paper, we provide numerical examples showing that the solution to the relaxed convex problem may fail to satisfy the original nonconvex constraints at one, multiple, or even all temporal grid points. These examples highlight potential challenges in directly extending lossless convexification from continuous-time to discrete-time settings.

Motivated by these observations, the primary goal of this paper is to develop a rigorous theoretical framework for directly applying lossless convexification to discrete-time nonconvex optimal control problems. Specifically, we provide formal reasoning to explain why constraint violations occur in discrete-time settings and establish theoretical bounds on the number of temporal grid points at which these violations can appear.

Instead of considering a general class of nonconvex control constraints, we focus on a simple problem where the lower bound of the nonzero norm on the control input magnitude is the sole source of nonconvexity. Here, the input magnitude is defined by a convex function of the input variable. We chose this problem because it can demonstrate the essence of LCvx method without introducing excessive mathematical complexity. The application of the LCvx method to a broader class of nonconvex problems will be explored in future studies.

In our theoretical framework for the discrete-time nonconvex problem, we classify such problems into two categories: normal cases and long-horizon cases. Long-horizon cases arise when the control horizon is sufficiently long to admit an optimal solution for the convexified problem, but the input magnitude of this solution consistently violates the nonconvex input constraints throughout the trajectory. All other problems are classified as normal cases. The existing LCvx method has demonstrated effective performance for normal cases [Açikmeşe and Ploen, 2005, 2007], but it fails for long-horizon cases because a key assumption for LCvx theory—the strict transversality assumption ([Malyuta et al., 2022, Condition 2], [Açikmeşe and Blackmore, 2011, Condition 2])—is no longer valid.

For the normal case, we provide a theoretical guarantee for applying the existing LCvx method to discrete-time optimal control problems by proving a bound on the number of points where the optimal solution to the convexified problem can violate the original nonconvex constraints. Specifically, we show that, after an arbitrarily small perturbation to the dynamics, the optimal solution to the convexified problem violates nonconvex con-

straints at no more than $n_x - 1$ temporal grid points, where n_x is the state dimension. Furthermore, we show that the perturbed problem maintains all necessary assumptions from the relaxed convex problem and we establish bounds on the impact of the perturbation. Numerical examples are also provided to demonstrate the necessity of the perturbation and the tightness of the upper bound. Our proof technique is closely related to the discretized Pontryagin’s Maximum Principle [Sethi, 2021, Canon et al., 1970], as both approaches are based on the Lagrangian function for finite-dimensional optimal control problems. However, unlike the discretized Pontryagin’s Maximum Principle, our method does not involve the use of the Hamiltonian.

In contrast, the existing LCvx method does not work for long-horizon cases because the strict transversality assumptions ([Malyuta et al., 2022, Condition 2], [Açikmeşe and Blackmore, 2011, Condition 2]) required by existing LCvx methods no longer hold for such cases. To address this, we propose a modification of the LCvx method by combining it with a bisection search. Specifically, we divide the control horizon into two phases. In the first phase, we use an arbitrary feasible control input to minimize cost. The final state of the first phase is then used as the initial state for the second phase, where we apply the existing LCvx method to the resulting nonconvex optimal control problem. We expect the control horizon for the second phase to be short enough to satisfy the transversality assumption and fall into the normal case category, while still being long enough to maintain minimum input cost. To achieve this balance, we develop a bisection search to determine the optimal transition time between phases, leveraging the continuity of the value function of the resulting convex optimal control problem. By employing a bisection search, the second-phase control problem falls into the normal case category, enabling us to directly apply the theoretical results of normal cases to long-horizon problems.

We note that other methods also address cases where the strict transversality assumptions no longer hold. For instance, [Kunhippurayil et al., 2021] applies a bisection search in continuous-time settings. Our work differs from [Kunhippurayil et al., 2021] by focusing on discrete-time problems, incorporating terminal costs into the objective rather than fixed terminal states, and performing the bisection search on a different, more practical discrete-time objective. Another long-horizon approach, presented in [Yang et al., 2024], introduces auxiliary state variables to indirectly address the issue. In contrast, we explicitly analyze why LCvx fails in long-horizon scenarios and propose a direct solution requiring fewer assumptions. This solution transforms the long-horizon problem into a normal one, allowing us to directly apply theoretical results developed for normal cases and facilitating extensions to other discrete-time LCvx methods, such as [Malyuta and Açikmeşe, 2020].

Statement of Contributions: In this paper, we develop a new LCvx theoretical framework that directly

applied to discrete-time nonconvex optimal control problems, bridging the gap between LCvx theory and its real-world applications. Specifically, our contributions are as follows.

First, we develop a new theoretical framework for discrete-time optimal control problems, which differs from previous LCvx research and other asymptotic theories for discretizations of continuous-time optimal control [Ober-Blöbaum et al., 2011, Lee et al., 2022]. By focusing on discrete-time settings, we can provide a tight upper bound for the number of temporal grid points at which the optimal control violates the non-convex constraints after applying the LCvx method.

Second, our theoretical framework employs linear algebra and finite-dimensional convex analysis, thus avoiding the need for infinite-dimensional mathematical tools such as Pontryagin’s maximum principle. This approach not only simplifies the theoretical development but also offers a fresh perspective on the mechanism of LCvx.

Third, our theoretical framework eliminates the requirement for the strict transversality assumption found in earlier LCvx theories ([Malyuta et al., 2022, Condition 2] and [Açikmeşe and Blackmore, 2011, Condition 2]), an assumption that is often difficult to verify before computation. This removal makes our LCvx theory more applicable to real-world applications.

Road map: In Section 2, we review the background of LCvx research and define the optimization problem under consideration. Next, in Section 3, we provide an intuitive explanation of the mechanism of LCvx using convex analysis techniques and define the mathematical criteria for normal cases and long-horizon cases. In Section 4, we discuss the validity of LCvx for normal cases, define perturbations to the discrete dynamics, and provide theoretical guarantees for the LCvx method on the perturbed nonconvex optimal control problem. In Section 5, we address the long-horizon case and propose a bisection search algorithm for these cases. Finally, in Section 6, we present numerical experiments to demonstrate counterexamples where the LCvx method is invalid and showcase the perturbation and bisection search algorithms.

1.1 Notation

In the remainder of this discussion, we adopt the following notation. The set of integers $\{a, a+1, \dots, b-1, b\}$ is denoted by $[a, b]_{\mathbb{N}}$. The set of real numbers is denoted by \mathbb{R} , the set of real $n \times m$ matrices by $\mathbb{R}^{n \times m}$, and the set of real n -dimensional vectors by \mathbb{R}^n . Vector inequalities are defined elementwise. For matrices A_1, A_2, \dots, A_n , where each matrix A_i has the same number of rows, we denote the horizontal concatenation of these matrices by (A_1, A_2, \dots, A_n) . This operation results in a matrix formed by placing matrices A_1 through A_n side by side, from left to right. The Euclidean norm for vectors and matrices is denoted by $\|\cdot\|$, and the absolute value by $|\cdot|$. For a matrix A , $\exp(A)$ denotes the matrix exponential of A , with the definition available in [Chen, 1984] and

$\text{rank}(A)$ denotes the rank of matrix A . For a convex set \mathbb{D} , the normal cone at the point z is denoted by $N_{\mathbb{D}}(z)$, with the definition found in [Borwein and Lewis, 2006, Chapter 2.1]. For a function $f(x, y)$ convex in (x, y) , $\partial_x f(x, y)$ and $\partial_y f(x, y)$ represent the subgradient of f with respect to the variables x and y separately, as defined in [Boyd and Vandenberghe, 2004]. For a differentiable function $f(x, y)$, $\nabla_x f(x, y)$ and $\nabla_y f(x, y)$ denote the partial derivative of f with respect to x and y separately. Finally, $\text{Prob}(E)$ denotes the probability that certain events E occur.

2 Background

In this section, we discuss the background of the LCvx method. Consider the optimization problem mentioned in [Malyuta et al., 2022, Problem 6], which includes no state constraints other than boundary conditions. We further simplify this problem to a time-invariant linear system without external disturbances. We believe that this basic form captures the essential ideas of the LCvx method without adding mathematical complexity. This leads to the following optimal control problem:

Problem 1:

$$\begin{aligned} \min_{t_f, u, x} \quad & m(x(t_f)) + \int_0^{t_f} l_c(g(u(t))) dt, \\ \text{s. t.} \quad & \dot{x}(t) = A_c x(t) + B_c u(t), \\ & \rho_{\min} \leq g(u(t)) \leq \rho_{\max}, \text{ for } t \in [0, t_f] \\ & x(0) = x_{\text{init}}, \quad G(x(t_f)) = 0. \end{aligned}$$

Here, $m: \mathbb{R}^{n_x} \rightarrow \mathbb{R}$, $l_c: \mathbb{R} \rightarrow \mathbb{R}$, and $g: \mathbb{R}^{n_u} \rightarrow \mathbb{R}$ are assumed to be convex C^1 smooth functions. $G: \mathbb{R}^{n_x} \rightarrow \mathbb{R}^{n_g}$ is an affine map. The state trajectory $x: [0, t_f] \rightarrow \mathbb{R}^{n_x}$ and the control input trajectory $u: [0, t_f] \rightarrow \mathbb{R}^{n_u}$ satisfy a continuous ordinary differential equation constraint. The condition $G(x(t_f)) = 0$ represents the boundary condition for the state trajectory x . $A_c \in \mathbb{R}^{n_x \times n_x}$ and $B_c \in \mathbb{R}^{n_x \times n_u}$ are constant matrices. $t_f \in \mathbb{R}$ is a free flight time and $x_{\text{init}} \in \mathbb{R}^{n_x}$ is a fixed initial state. $\rho_{\min} \in \mathbb{R}$ and $\rho_{\max} \in \mathbb{R}$ are fixed constants. The nonconvexity of Problem 1 arises solely from potentially nonconvex constraints $\rho_{\min} \leq g(u(t))$, where g characterizes the magnitude of the input variable. A classic realization of g is to use the norm function. Such constraints arise from planetary soft landing applications, where the net thrust of rocket engines must exceed a positive lower bound to prevent shutdown [Açikmeşe and Ploen, 2005].

The LCvx technique introduced in [Açikmeşe and Blackmore, 2011] considers the following convex relaxation of the Problem 1:

Problem 2:

$$\begin{aligned} \min_{t_f, \sigma, u, x} \quad & m(x(t_f)) + \int_0^{t_f} l_c(\sigma(t)) dt \\ \text{s. t.} \quad & \dot{x}(t) = A_c x(t) + B_c u(t) \\ & \rho_{\min} \leq \sigma(t) \leq \rho_{\max}, \quad g(u(t)) \leq \sigma(t) \\ & x(0) = x_{\text{init}}, \quad G(x(t_f)) = 0 \end{aligned}$$

where $\sigma: [0, t_f] \rightarrow \mathbb{R}$ is a slack variable. The introduction of the slack variable σ makes the feasible set convex. Under mild conditions, the dual variables associated with the constraint $g(u(t)) \leq \sigma(t)$ are positive almost everywhere, enforcing the equality $g(u(t)) = \sigma(t)$ for almost every t , as formally established in Theorem [Açikmeşe and Blackmore, 2011, Theorem 2]. Consequently, the solution to the convexified problem satisfies the original nonconvex constraint $\rho_{\min} \leq g(u(t)) \leq \rho_{\max}$ for almost every t .

Now, we consider the discretized, finite-dimensional, versions of Problem 1 and Problem 2. We apply a temporal discretization with zero-order hold for both infinite-dimensional problems to solve them numerically [Açikmeşe and Ploen, 2005, 2007, Açikmeşe and Blackmore, 2011]. Meanwhile, having a free final time t_f can undermine the convexity of the resulting optimization problem. To address this, a commonly used method is to apply a line search for t_f . By solving the discretized relaxed problem for each t_f , one can find a t_f with the smallest objective value [Açikmeşe and Ploen, 2007]. Hence, in the rest of this paper, we only consider the cases where t_f is fixed.

With the following solution variables:

$$\begin{aligned} x &= \{x_1, x_2, \dots, x_{N+1}\}, \quad x_i \in \mathbb{R}^{n_x} \text{ for } i \in [1, N+1]_{\mathbb{N}} \\ u &= \{u_1, u_2, \dots, u_N\}, \quad u_i \in \mathbb{R}^{n_u} \text{ for } i \in [1, N]_{\mathbb{N}} \\ \sigma &= \{\sigma_1, \sigma_2, \dots, \sigma_N\}, \quad \sigma_i \in \mathbb{R} \text{ for } i \in [1, N]_{\mathbb{N}}. \end{aligned}$$

The discretized version of Problem 1 is:

Problem 3:

$$\begin{aligned} \min_{x, u} \quad & m(x_{N+1}) + \sum_{i=1}^N l_i(g(u_i)) \\ \text{s. t.} \quad & x_{i+1} = A_d x_i + B_d u_i, \quad i \in [1, N]_{\mathbb{N}} \\ & \rho_{\min} \leq g(u_i) \leq \rho_{\max}, \quad i \in [1, N]_{\mathbb{N}} \\ & x_1 = x_{\text{init}}, \quad G(x_{N+1}) = 0. \end{aligned}$$

The sum of $l_i: \mathbb{R} \rightarrow \mathbb{R}$ is an approximation for the integral term in the objective function of Problem 1. Matrices $A_d \in \mathbb{R}^{n_x \times n_x}$ and $B_d \in \mathbb{R}^{n_x \times n_u}$ for this discretized problem are given as [Chen, 1984]:

$$A_d = \exp\left(A_c \frac{t_f}{N}\right), \quad B_d = \int_0^{t_f/N} \exp(A_c \tau) d\tau B_c \quad (1)$$

Since we mainly work with the discretized problem, we simplify the notation by using A for A_d and B for B_d . Condition $G(x_{N+1}) = 0$ is denoted as the boundary condition, $x_{i+1} = Ax_i + Bu_i$ as the dynamics constraints, and $m(x_{N+1}) + \sum_i l_i(\sigma_i)$ as the object function.

The discretized version of Problem 2 is:

Problem 4:

$$\begin{aligned} \min_{x, u, \sigma} \quad & m(x_{N+1}) + \sum_{i=1}^N l_i(\sigma_i) \\ \text{s. t.} \quad & x_{i+1} = Ax_i + Bu_i, \quad i \in [1, N]_{\mathbb{N}} \\ & \rho_{\min} \leq \sigma_i \leq \rho_{\max}, \quad g(u_i) \leq \sigma_i, \quad i \in [1, N]_{\mathbb{N}} \\ & x_1 = x_{\text{init}}, \quad G(x_{N+1}) = 0. \end{aligned}$$

Problem 4 can be understood as the result of applying the LCvx method to Problem 3. Since Problem 4 is a relaxation of Problem 3, its optimal value serves as a lower bound for that of Problem 3.

Motivated by previous LCvx research on continuous problems, a natural question arises: does the optimal solution to Problem 4 satisfy the constraints of Problem 3? However, this relationship does not hold in general. The numerical counterexamples in Section 6 show that the solution to Problem 4 often does not satisfy the constraints of Problem 3 at certain temporal grid points. Therefore, an optimal solution to Problem 4 is not guaranteed to solve Problem 3. As a result, we shifted our focus to a revised question. At how many temporal grid points can the solution to Problem 4 potentially violate the constraints of Problem 3, thereby invalidating LCvx? Here, we define the validity of LCvx at grid point i as:

Definition 1 *The LCvx method is valid at a grid point i if the control input u_i satisfies $\rho_{\min} \leq g(u_i) \leq \rho_{\max}$.*

We will later prove that, with reasonable assumptions on Problem 4 and with arbitrarily small random perturbations to the discrete dynamics, LCvx is invalid at most at $n_x - 1$ temporal grid points, where n_x denotes the dimension of the variable x .

Before the theoretical discussion, we provide some definitions and assumptions for the problem 4 required for our discussion.

Assumption 2 *$l_i(\cdot)$ is C^1 smooth and monotonically increasing on $[\rho_{\min}, \infty)$. The function m is also C^1 smooth. The set $\{u \mid g(u_i) \leq \rho_{\min} \text{ for all } i\}$ is nonempty, and the set $\{u \mid g(u_i) \leq \rho_{\max} \text{ for all } i\}$ is compact.*

We also require that the dynamical system in Problem 4 is controllable. Note that the controllability of the discretized system is closely related to that of the continuous system [Chen, 1984, Theorem 6.9].

Assumption 3 (Controllability) *For matrices A and B in Problem 4,*

$$\text{rank} \begin{pmatrix} B & AB & \dots & A^{n_x-1}B \end{pmatrix} = n_x,$$

i.e., the matrix pair $\{A, B\}$ is controllable.

We now introduce some notation for further assumptions. Since the constraints on (u, σ) in Problem 4 are identical at each temporal grid point, we define

$V := \{(\bar{u}, \bar{\sigma}) \in \mathbb{R}^{n_u} \times \mathbb{R} \mid \rho_{\min} \leq \bar{\sigma} \leq \rho_{\max}, g(\bar{u}) \leq \bar{\sigma}\}$, so that the constraint in Problem 4 can be expressed as $(u_i, \sigma_i) \in V$ for all i . Since g is convex, the set V is a convex set.

Moreover, we define $V(\cdot)$ as $V(\bar{\sigma}) := \{\bar{u} \in \mathbb{R}^{n_u} \mid g(\bar{u}) \leq \bar{\sigma}\}$, i.e. $V(\bar{\sigma})$ is a slice of V at a specific value of $\bar{\sigma} \in \mathbb{R}$. The definition of $V(\cdot)$ establishes a sufficient condition for the validity of LCvx for certain u_i . The following lemma follows immediately.

Lemma 4 *Under Assumption 2, if a control \bar{u} lies on the boundary of $V(\bar{\sigma})$, \bar{u} satisfies the constraints in Problem 3, i.e. $\rho_{\min} \leq g(\bar{u}) = \bar{\sigma} \leq \rho_{\max}$.*

To define other assumptions, we need to further simplify the notation for Problem 4. Let $z := (x, u, \sigma) \in \mathbb{R}^{n_z}$ with $n_z = (N+1)n_x + Nn_u + N$. We denote the object function as $\Phi: \mathbb{R}^{n_z} \rightarrow \mathbb{R}$ and encapsulate the dynamics and boundary conditions into an affine constraint $H(z) = 0$, where $H: \mathbb{R}^{n_z} \rightarrow \mathbb{R}^{n_H}$ and n_H represents the total number of equality constraints. The remaining inequality constraints are written within the convex set $\tilde{V} = \{(x, u, \sigma) \in \mathbb{R}^{n_z} \mid (u_i, \sigma_i) \in V \text{ for all } i\}$. Thus, Problem 4 can be represented as:

Problem 5:

$$\begin{aligned} \min_z \quad & \Phi(z) \\ \text{s. t.} \quad & H(z) = 0, \quad z \in \tilde{V}. \end{aligned}$$

Since H is an affine function, the Jacobian of H , denoted as $\nabla H(z)$, is a constant matrix. Therefore, by eliminating the equations in H if necessary, $\nabla H(z)$ becomes a matrix of full rank. Since the dynamics equalities are designed to be full rank, any elimination of redundant constraints occurs only at the boundary condition and does not affect the dynamics equalities. After this elimination, we make the following assumption:

Assumption 5 For Problem 5, $\nabla H(z)$ has full row rank.

For the convex Problem 5, we further require the Slater condition:

Assumption 6 (Slater's condition) For Problem 5, there exists a vector z in the interior of \tilde{V} such that $H(z) = 0$

Assumption 6 is relatively modest. When g is the Euclidean norm function, Assumption 6 is equivalent to having a control sequence $\|u_i\| < \rho_{max}$ such that the trajectory generated by this u_i satisfies $G(x_{N+1}) = 0$. This holds when the optimal control problem is not overly constrained.

In the following discussion of this paper, Assumption 2, 3, 5, and 6 are valid for Problem 4 without further mentioning.

We conclude the background section with a continuity theorem, which is a major tool in our subsequent theoretical discussion. We begin by introducing a lemma which is a direct consequence of [Clarke et al., 2008, Lemma 3.3.3, Theorem 3.3.4]:

Lemma 7 Consider an optimization problem **Problem 6:**

$$\begin{aligned} \min_y \quad & M(y, p) \\ \text{s. t.} \quad & F(y, p) = 0, \quad y \in \Omega, \end{aligned}$$

where $y \in \mathbb{R}^{n_y}$, $p \in \mathbb{R}^{n_p}$. $M: \mathbb{R}^{n_y+n_p} \rightarrow \mathbb{R}$ and $F: \mathbb{R}^{n_y+n_p} \rightarrow \mathbb{R}^{n_F}$ are continuous with respect to (y, p) , and $\nabla_y F$ exists and is continuous with respect to (y, p) . Consider a solution (y^*, p_0) to the equality/constraint system

$$F(y^*, p_0) = 0, \quad y^* \in \Omega,$$

such that $\eta = 0$ is the unique solution to the following

equation

$$0 \in \nabla_y F(y^*, p_0)^\top \eta + N_\Omega(y^*).$$

Then, there exist $\delta, \xi > 0$ such that for any $p \in \mathbb{R}^{n_p}$ with $\|p - p_0\| < \xi$, there is a point $y \in \Omega$ satisfying $F(y, p) = 0$ and

$$\|y - y^*\| \leq \frac{\|F(y^*, p)\|}{\delta}.$$

We denote the optimum value to Problem 6 as $M^*(p)$. Our goal here is to show the continuity of M^* .

Theorem 8 Assume that the function F and an optimal solution (y^*, p_0) to Problem 6 satisfy all the assumptions in Lemma 7, Ω is compact, and M is a locally Lipschitz function with respect to (y, p) . Then, The optimal value function $M^*: \mathbb{R}^{n_p} \rightarrow \mathbb{R}$ to Problem 6 is continuous at p_0 .

PROOF. See Appendix 8.1. \square

3 Mechanism of LCvx

In this section, we provide a sufficient condition for the validity of LCvx and introduce the long-horizon cases and the normal cases for Problem 4.

To start, we define the Lagrangian of Problem 4 as follows:

$$\begin{aligned} L(x, u, \sigma; \eta, \mu_1, \mu_2) := & m(x_{N+1}) + \sum_{i=1}^N I_V(u_i, \sigma_i) \\ & + \sum_{i=1}^N l_i(\sigma_i) + \sum_{i=1}^N \eta_i^\top (-x_{i+1} + Ax_i + Bu_i) \\ & + \mu_1^\top (x_1 - x_{init}) + \mu_2^\top G(x_{N+1}), \end{aligned}$$

where I_V is the indicator function of set V :

$$I_V(\bar{u}, \bar{\sigma}) = \begin{cases} 0 & \text{if } (\bar{u}, \bar{\sigma}) \in V, \\ +\infty & \text{otherwise,} \end{cases}$$

and the dual variable $\eta_i \in \mathbb{R}^{n_x}$ for $i = 1, 2, \dots, N$, $\eta = [\eta_1^\top, \eta_2^\top, \dots, \eta_N^\top]^\top \in \mathbb{R}^{n_x N}$, $\mu_1 \in \mathbb{R}^{n_x}$, and $\mu_2 \in \mathbb{R}^{n_G}$.

Theorem 9 Suppose Assumption 6 holds, and let (x^*, u^*, σ^*) be a solution of Problem 4. Then, there exist dual variables $(\eta^*, \mu_1^*, \mu_2^*)$ such that

$$(x^*, u^*, \sigma^*) = \arg \min_{x, u, \sigma} L(x, u, \sigma; \eta^*, \mu_1^*, \mu_2^*). \quad (2)$$

PROOF. This follows directly from [Clarke, 2013, Theorem 9.4, 9.8 and 9.14]. \square

From equation (2), we derive:

$$\begin{aligned} \sigma^* &= \arg \min_{\sigma} L(x^*, u^*, \sigma; \eta^*, \mu_1^*, \mu_2^*), \\ u^* &= \arg \min_u L(x^*, u, \sigma^*; \eta^*, \mu_1^*, \mu_2^*), \\ x^* &= \arg \min_x L(x, u^*, \sigma^*; \eta^*, \mu_1^*, \mu_2^*). \end{aligned} \quad (3)$$

Since in the Lagrangian L , u_i only appears in terms $I_V(u_i, \sigma_i)$ and $\eta_i^\top Bu_i$, we can write:

$$\begin{aligned} u_i^* &= \arg \min_{u_i} I_V(u_i, \sigma_i^*) + \eta_i^{*\top} Bu_i \\ &= \arg \min_{u_i} I_{V(\sigma_i^*)}(u_i) + \eta_i^{*\top} Bu_i. \end{aligned} \quad (4)$$

Equation (4) characterizes the relationship between u_i^* and σ_i^* . With (4) in hand, we discuss the sufficient condition for LCvx to be valid.

Theorem 10 (Sufficient Condition for LCvx)

Under Assumptions 2 and 6, the condition of $-B^\top \eta_i^*$ being nonzero is sufficient for u_i to lie on the boundary of $V(\sigma_i^*)$, thus validating LCvx at the grid point i by Lemma 4. Furthermore, η_i^* is given by $\eta_i^* = A^{\top(N-i)} \eta_N^*$.

PROOF. We first address the sufficient condition for u_i^* to lie on the boundary of $V(\sigma_i^*)$. Given that the right-hand side function of equation (4) is convex in u_i and u_i^* is a minimizer of this convex function, it follows that [Borwein and Lewis, 2006, Proposition 2.1.2]

$$-B^\top \eta_i^* \in N_{V(\sigma_i^*)}(u_i^*),$$

where $N_{V(\sigma_i^*)}(u_i)$ denotes the normal cone of the set $V(\sigma_i^*)$ at point u_i^* . The normal cone has nonzero elements only at the boundary points of $V(\sigma_i^*)$ [Bauschke, 2011, Corollary 6.44]. Hence, $-B^\top \eta_i^*$ being nonzero implies that u_i lies on the boundary of $V(\sigma_i^*)$. In such a case, LCvx is valid at node i according to Lemma 4.

For the evolution of η_i , considering equation (3), we take the partial derivative of L with respect to x_i for all i , yielding:

$$x_{N+1}: \quad \nabla m(x_{N+1}) + \mu_2^\top \nabla G(x_{N+1}) = \eta_N^*, \quad (5a)$$

$$x_i: \quad \eta_i^{*\top} A - \eta_{i-1}^{*\top} = 0, \quad (5b)$$

$$x_1: \quad \mu_1^\top + \eta_1^{*\top} A = 0.$$

Thus, iteratively applying (5b) leads to $\eta_i^* = A^{\top(N-i)} \eta_N^*$. \square

Remark 11 Theorem 10 offers insight into why discrete LCvx is typically valid in applications. We start by designing a slack variable σ such that for a fixed σ , LCvx is valid as long as the control u is on the boundary of the feasible region defined by σ . Then, if a dual variable η_i^* is not in the left null space of matrix B , the corresponding control u lies on the boundary of the feasible region, thus validating LCvx.

However, Theorem 10 does not guarantee the validity of LCvx, as $-B^\top \eta_i^* = 0$ can occur for some i . An obvious scenario for $\eta_i^* = 0$ is where $\eta_N^* = 0$. The following lemma characterizes this scenario.

Lemma 12 Under Assumptions 2 and 6, if $\eta_N^* = 0$, then all $\sigma_i^* = \rho_{\min}$, and x_{N+1} must be an optimal solution to the following optimization problem:

Problem 7:

$$\begin{aligned} \min_z \quad & m(x_{N+1}) \\ \text{s. t.} \quad & G(x_{N+1}) = 0. \end{aligned}$$

PROOF. From Theorem 10, $\eta_N^* = 0$ implies $\eta_i^* = 0$ for all i . By Theorem 9, we have

$$(\sigma^*, u^*) = \arg \min_{\sigma, u} \sum_{i=1}^N l_i(\sigma_i) + \sum_{i=1}^N I_V(u_i, \sigma_i).$$

Given Assumption 2, we have that $\sigma_i^* = \rho_{\min}$ and $u_i \in V(\rho_{\min})$.

We now prove the result on x_{N+1} . Equation (5a) ensures that

$$\nabla m(x_{N+1}) + \mu_2^\top \nabla G(x_{N+1}) = \eta_N^* = 0,$$

indicating that x_{N+1} is a KKT point of the convex optimization Problem 7 and thus a minimizer [Borwein and Lewis, 2006]. \square

Theorem 10 provides a sufficient condition for $\eta_N^* \neq 0$, leading to a natural division of Problem 4 into two scenarios:

Definition 13 Problem 4 is defined as the long-horizon case if $\sigma_i^* = \rho_{\min}$ and x_{N+1} solves Problem 7. If these conditions are not satisfied, Problem 4 is classified as the normal case.

The term long-horizon is used because $\eta_N^* = 0$ typically occurs when the control horizon is large. For a problem in the normal case, $\eta_N^* \neq 0$ according to Lemma 12. In previous LCvx research, $\eta_N^* \neq 0$ is usually ensured by assumptions, for example [Malyuta et al., 2022, Condition 2] and [Açikmeşe and Blackmore, 2011, Condition 2]. By identifying the long-horizon case, we can omit such types of assumptions.

In the next section, we discuss the theoretical guarantee for normal cases. The long-horizon cases will be left for the subsequent section.

4 LCvx on Normal cases

In this section, we concentrate on problems in the normal case and thus we assume that

Assumption 14 Problem 4 is normal, i.e., either $\sigma_i > \rho_{\min}$ for some i or x_{N+1} is not the minimizer for Problem 7.

As discussed previously, Assumption 14 implies that $\eta_N^* \neq 0$. A direct consequence of this assumption is:

Corollary 15 Given Assumptions 2, 6 and 14, if the matrix A and B are invertible, then LCvx is valid at all temporal grid points.

PROOF. When $\eta_N^* \neq 0$, since $\eta_i^* = A^{\top(N-i)} \eta_N^*$, a full rank matrix A ensures that η_i^* is non-zero for all i . The invertibility of B implies that $\eta_i^{*\top} B$ is non-zero for every i , satisfying the conditions of Theorem 10 for LCvx to hold. \square

However, Corollary 15 might not always be applicable because it requires matrix B to be a square matrix, which means that the control and state dimensions must be equal; In practice, the state dimension often significantly exceeds the control dimension.

When the state dimension is larger than the control dimension, the validity of LCvx at all grid points is not guaranteed. Numerical examples in Section 6 show the invalidity of LCvx at multiple grid points for a non-square matrix B , even when the LCvx problem is normal. Therefore, we aim to establish a weaker statement:

the original nonconvex constraints are violated at most at $n_x - 1$ temporal grid points, where n_x is the state dimension. However, this statement is still invalid as counterexamples exist (see Section 6.2). Thus, we consider an even weaker statement: after adding a random perturbation to the dynamics matrix A in Problem 4, the nonconvex constraints are violated at no more than $n_x - 1$ temporal grid points.

4.1 Perturbation

We define an arbitrarily small perturbation in the context of matrix A 's Jordan form, where A is defined in the dynamics constraints of Problem 3 and Problem 4:

Definition 16 Let matrix A 's Jordan form be

$$A = Q^{-1} J Q.$$

Let $\{\lambda_1, \dots, \lambda_d\}$ be the set of all distinct eigenvalues of A . Define $\tilde{A}(q)$ as a perturbation of A with respect to a vector $q = (q_1, q_2, \dots, q_d) \in \mathbb{R}^d$ if:

- $\tilde{A}(q) = Q^{-1} \tilde{J} Q$, where \tilde{J} is a Jordan matrix that is identical to J except for its diagonal elements.
- $\tilde{A}(q)$ has d eigenvalues $(\tilde{\lambda}_1, \dots, \tilde{\lambda}_d)$ such that $(\tilde{\lambda}_1, \dots, \tilde{\lambda}_d) = (\lambda_1, \lambda_2, \dots, \lambda_d) + (q_1, q_2, \dots, q_d)$.
- The index of Jordan blocks in \tilde{J} corresponding to $\tilde{\lambda}_i$ remains the same as in J corresponding to λ_i .

In essence, perturbing a matrix involves altering its eigenvalues. We intentionally preserve the Jordan form as it may convey important structural information about the dynamical system.

We now perturb Problem 4 by replacing the matrix A in the dynamic constraints with $\tilde{A}(q)$, where $\tilde{A}(q)$ represents a perturbation of A with respect to the vector $q \in \mathbb{R}^d$. Consequently, the optimization problem can be reformulated as follows:

Problem 8:

$$\begin{aligned} \min_{x, u, \sigma} \quad & m(x_{N+1}) + \sum_{i=1}^N l_i(\sigma_i) \\ \text{s. t.} \quad & x_{i+1} = \tilde{A}(q)x_i + Bu_i, \quad i \in [1, N]_{\mathbb{N}} \\ & \rho_{\min} \leq \sigma_i \leq \rho_{\max}, \quad g(u_i) \leq \sigma_i, \quad i \in [1, N]_{\mathbb{N}} \\ & x_1 = x_{\text{init}}, \quad G(x_{N+1}) = 0. \end{aligned}$$

If $q = 0$, we restore Problem 4.

In the remainder of this paper, $\mathbb{D} \subset \mathbb{R}^n$ denotes an n -dimensional unit cube, defined as $\mathbb{D} = \{x \in \mathbb{R}^n \mid -1 \leq x_i \leq 1, \forall i = 1, \dots, n\}$, where x_i is the i -th component of x in \mathbb{R}^n . For $\epsilon > 0$, we define the scaled cube $\epsilon\mathbb{D}$ as $\{x \in \mathbb{R}^n \mid -\epsilon \leq x_i \leq \epsilon, \forall i = 1, \dots, n\}$. The following theorem ensures that Assumptions 3, 5, 6, and 14 remain valid for the perturbed problem 8 under sufficiently small perturbations $q \in \epsilon\mathbb{D}$.

Lemma 17 Suppose that Assumptions 2, 3, 5, 6 and 14 hold for Problem 8 when $q = 0$. Then there exists an $\epsilon > 0$ such that for any $q \in \epsilon\mathbb{D} \subset \mathbb{R}^d$, these assumptions still hold for Problem 8 after perturbation by q .

PROOF. See Appendix 8.2. \square

Remark 18 In Lemma 17, we choose q from a cube region instead of the more conventional ball region, because we later want to generate q via a uniform distribution, and the cube region ensures independence for each dimension of q .

Lemma 17 establishes that Problem 8 follows the same assumptions as Problem 4. Therefore, all discussions in Section 3 regarding Problem 4 are also applicable to Problem 8 for sufficiently small q .

4.2 Quantify the LCvx invalidation

The goal for this section is to demonstrate that when the perturbation q is chosen randomly, the probability that LCvx is invalid for problem 8 at no more than $n_x - 1$ points is zero. To begin, we examine the necessary conditions for Problem 8 to violate the original nonconvex constraints at the grid points indexed by $P_1, P_2, \dots, P_k \in \mathbb{N}$.

Lemma 19 For Problem 8 with a fixed perturbation q , we define

$$S = \begin{pmatrix} \tilde{A}(q)^{N-P_1} B & \tilde{A}(q)^{N-P_2} B & \dots & \tilde{A}(q)^{N-P_k} B \end{pmatrix},$$

where $P_1, P_2, \dots, P_k \in \mathbb{N}$ are temporal grid points. Suppose that Assumptions 2, 6, and 14 hold for Problem 8. If LCvx is invalid at the temporal grid points $P_1, P_2, \dots, P_k \in \mathbb{N}$, then the rank of S satisfies $\text{rank}(S) < n_x$.

PROOF. According to Theorem 10, the necessary condition for LCvx to be violated at the i -th point is: $\eta_i^\top B = 0$. Given that $\eta_i^\top = \eta_N^\top \tilde{A}(q)^{N-i}$, it follows that η_N^\top must lie in the left null space of $\tilde{A}(q)^{N-i} B$. Consequently, if LCvx is invalid at $\{P_1, P_2, \dots, P_k\}$, η_N^\top must lie in the left null space of the matrix S . According to Assumption 14, η_N is nonzero. Hence S has nontrivial left null space. Then $\text{rank}(S) < n_x$. \square

Now we have the main theorem.

Theorem 20 Given that Assumptions 2, 5, 6 and 14 hold for Problem 4, along with the controllability of $\{A, B\}$. Then, there exists an $\epsilon > 0$ such that if a vector $q \in \mathbb{R}^d$ is uniformly distributed over cube $\epsilon\mathbb{D} \in \mathbb{R}^d$, the probability of the optimal trajectory for Problem 8 violating the nonconvex constraints in Problem 3 at more than $n_x - 1$ grid points is zero.

PROOF. See Appendix 8.3. The key to this proof is to use Lemma 19. We show that for a sufficiently small perturbation q and for arbitrary integers $1 \leq P_1 < P_2 < \dots < P_{n_x} < N + 1$, where N is the total amount of temporal grid points, the matrix S defined in Lemma 19 is of full rank with probability one. \square

We also want to estimate the influence of the perturbation. Taking the control sequence that is optimum to Problem 8, and applying it to the unperturbed dynamics, we are expecting that when perturbation q is sufficiently small, the perturbation does not lead to a

significant difference in the output of the unperturbed dynamics.

Theorem 21 Suppose Assumptions 2, 5, 6 and 14 hold for Problem 8. Let the control sequence obtained by solving Problem 8 as $u(q)$ and apply this control to the unperturbed dynamics, leading to a trajectory

$$\begin{aligned}\bar{x}_{N+1}(q) &= x_1 + \sum_{i=1}^N A^{i-1} B u_i(q) \\ &= x_1 + \sum_{i=1}^N \bar{A}^{i-1}(0) B u_i(q)\end{aligned}$$

where $u_i(q)$ is the control sequence $u(q)$ at the i -th temporal grid point. Then, for any $\delta > 0$, there exists an $\epsilon > 0$ such that for any $\|q\| < \epsilon$, $\bar{x}_{N+1}(q)$ and $u(q)$ satisfy:

- $\|G(\bar{x}_{N+1}(q))\| \leq \delta$,
- $m(\bar{x}_{N+1}(q)) + \sum_{i=1}^N l_i(g(u_i(q))) \leq m_o^* + \delta$,

where m_o^* is the optimum value of the discretized non-convex Problem 3.

PROOF. See Appendix 8.4. \square

Remark 22 The perturbation mentioned in Theorem 20 is introduced solely for mathematical discussion and is **not required** in practical applications. Nevertheless, it is mathematically necessary: the numerical example in Section 6, constructed as a counterexample, demonstrates that LCvx can become invalid at more than $n_x - 1$ nodes if no perturbation is applied, and it indicates that $n_x - 1$ is a tight upper bound for the number of temporal grid points at which LCvx becomes invalid when the control dimension is one. In such deliberately constructed cases, any perturbation that meets the following two requirements is sufficient: it must be small enough to avoid significantly affecting the final state (as ensured by Theorem 21) and large enough to be detected by the optimization algorithm. In our numerical implementation, we select a perturbation magnitude that is significantly larger than the solver's effective numerical precision, ensuring that it meaningfully influences the solution. We then re-run the convex solver for the perturbed problem to obtain the final result.

Our theoretical results guarantee at most $n_x - 1$ violations of control constraints, which may still be problematic in practice. To resolve this, we propose a simple correction step. For illustration, consider $g(x) = \|x\|$ (extensions are straightforward). Define the corrected control:

$$\hat{u}_i = \begin{cases} u_i, & \|u_i\| \geq \rho_{\min} \\ \rho_{\min} \frac{u_i}{\|u_i\|}, & \text{otherwise} \end{cases}$$

and let $\{\hat{x}_i\}$ be the resulting state trajectory.

Theorem 23 Given a uniform discretization t_f/N , the final-state deviation satisfies:

$$\|\hat{x}_{N+1} - x_{N+1}\| \leq (n_x - 1)C_0 \left(e^{\|A_c\| \frac{t_f}{N}} - 1 \right),$$

where C_0 depends on $\{A_c, B_c, \rho_{\min}\}$. If A_c is asymptotically stable, the bound tightens to:

$$\|\hat{x}_{N+1} - x_{N+1}\| \leq C_1 \frac{n_x - 1}{N},$$

where C_1 depends additionally on t_f .

PROOF. See Appendix 8.5.

Remark 24 Theorem 23 shows that the impact of violations decreases at a rate of $O(t_f/N)$, aligning with the continuous-time LCvx results as N approaches infinity. Thus, violations become negligible for sufficiently large N .

Practically, prior LCvx studies rarely encounter multiple violations, indicating that moderate discretization N often suffices. Hence, one may select a sufficiently large N based on theoretical bounds or adjust N adaptively, starting from a moderate initial value and increasing it if violations significantly impact the results. Solutions obtained at smaller discretizations can serve as warm starts for larger problems, thereby minimizing computational cost.

5 LCvx on Long-horizon Cases

In long-horizon cases, the optimal control inputs of Problem 4 may violate the nonconvex constraints of Problem 3 at all temporal grid points, i.e., $g(u_i) < \rho_{\min}$ for all i . Our goal is to find an optimal solution to the continuous-time nonconvex Problem 1 that minimizes both the control cost and boundary cost. If such a solution exists, its final state $x(t_f)$ should be the optimal solution to Problem 7, and the control input should satisfy $g(u) = \rho_{\min}$.

To solve the continuous-time nonconvex Problem 1, we divide the trajectory into two phases, with t_s as the switching point. The first phase is defined on the interval $[0, t_s]$. In this phase, we set the control input $u : [0, t_s] \rightarrow \mathbb{R}^{n_u}$ to be constant, ensuring that $g(u) = \rho_{\min}$, while the state trajectory follows the continuous dynamics described in Problem 1. The final state of the first phase then serves as the initial state for the second phase. In the second phase, we formulate a discrete-time convex optimization problem by discretizing the continuous dynamics over $[t_s, t_f]$. The boundary state constraint is maintained, and the convexified control constraints are evaluated at temporal grid points.

Determining the transition time t_s is challenging, as it must be large enough for the second phase optimization problem to belong to the normal cases, yet small enough to reduce the control and final state costs. Hence, we adopt the bisection search method to determine t_s . We will demonstrate that the optimal total cost of the first and second phases is a continuous function of t_s , which justifies the use of the bisection search method. An optimal t_s should minimize the total cost while ensuring that the discrete convex LCvx problem in the second phase is normal.

As explored in Section 4, solving the discrete LCVx problem does not ensure LCVx validation at all temporal grid points. Thus, we aim to find a control sequence such that the constraint $\rho_{\min} + \epsilon \geq g(u_i) \geq \rho_{\min}$ for an arbitrarily small fixed $\epsilon > 0$, with violations at no more than $n_x - 1$ grid points after the perturbation described in Theorem 20. Additionally, x_{N+1} should be an optimal solution to Problem 7 up to any arbitrarily small fixed constant ϵ . The mathematical definition for this statement is available in Theorem 30.

Now, we rigorously define the bisection search method. In the first phase, we fix the control input as a constant $u_s \in \mathbb{R}^{n_u}$ over a duration $t_s \in \mathbb{R}$, with the initial condition $x_s \in \mathbb{R}^{n_x}$ provided in the original problem. The control u_s is chosen to ensure $g(u_s) = \rho_{\min}$. The continuous dynamics matrices are denoted as A_c and B_c . By plugging in u_s into the continuous dynamics, we determine the final state of the first phase, which also serves as the initial condition for the second phase:

$$x_{\text{init}}(t_s) = \exp(A_c t_s) x_s + \int_0^{t_s} \exp(A_c \tau) d\tau B_c u_s.$$

For the second phase, we define a discrete convexified optimization Problem 4, keeping the dynamics discretized as N pieces with zero-order hold control. The discrete dynamics matrices are expressed as:

$$A(t_s) = \exp\left(A_c \frac{t_f - t_s}{N}\right),$$

$$B(t_s) = \int_0^{(t_f - t_s)/N} \exp(A_c \tau) d\tau B_c,$$

where $t_f - t_s$ is the amount of time remaining for the second phase.

Furthermore, we modify the objective function of Problem 4 by replacing $l_i(\sigma_i)$ with $l(\sigma_i) \times (t_f - t_s)/N$, where l is chosen such that its derivative on the domain of σ is lower-bounded by some $L_l > 0$. This adjustment simplifies the mathematical derivation. Theorem 30 justifies this modification, ensuring that the quality of the resulting trajectory and control variables remains unaffected.

The optimization problem for the second phase is then formulated as:

Problem 9:

$$\begin{aligned} \min_{x, u, \sigma} \quad & m(x_{N+1}) + \sum_{i=1}^N l(\sigma_i) \frac{t_f - t_s}{N} + t_s l(\rho_{\min}) \\ \text{s. t.} \quad & x_{i+1} = A(t_s)x_i + B(t_s)u_i, \text{ for } i \in [1, N]_{\mathbb{N}}. \\ & \rho_{\min} \leq \sigma_i \leq \rho_{\max}, \quad g(u_i) \leq \sigma_i, \text{ for } i \in [1, N]_{\mathbb{N}}. \\ & x_1 = x_{\text{init}}(t_s), \quad G(x_{N+1}) = 0. \end{aligned}$$

Here, we introduce a constant term $t_s l(\rho_{\min})$ to the objective function of the aforementioned optimization problem to account for the cost of the first phase. This addition simplifies the proof while leaving the optimal solution of the second phase unaffected. The value of the optimal objective function, denoted by $v(t_s)$, depends on t_s and represents the total cost of the flight, where the

minimum value of $v(t_s)$ is $m^* + t_{fl}(\rho_{\min})$, with m^* being the optimal value of Problem 7. Our primary objective is to determine a t_s such that $v(t_s) < m^* + t_{fl}(\rho_{\min}) + \epsilon$, for a given and arbitrarily small $\epsilon > 0$. Additionally, to ensure the applicability of the theorems from the previous section, we require that Problem 9 satisfies the normal case condition.

To simplify the notation for Problem 9, we define $z = (x, u, \sigma)$, the object function as $M(z, t_s)$, and all affine equalities as $F(z, t_s) = 0$. The remaining inequality constraints are identical to the set \tilde{V} in Problem 5. Thus, our problem can be represented as:

Problem 10:

$$\begin{aligned} \min_z \quad & M(z, t_s) \\ \text{s. t.} \quad & F(z, t_s) = 0, \quad z \in \tilde{V}. \end{aligned}$$

The optimal value is a function of t_s , denoted as $v(t_s)$.

We require the following assumption for Problem 10.

Assumption 25 *Problem 4 belongs to the long-horizon case. Meanwhile, there exists a t_b such that $v(t_b) > m^* + t_{fl}(\rho_{\min})$. Assumptions 2, 3, 5, and 6 are valid for Problem 10 generated by $t_s \in [0, t_b]$.*

Lemma 26 *Assumption 25 ensures that Problem 10 generated by t_b has a non-zero η_N^* .*

PROOF. The condition $v(t_b) > m^* + t_{fl}(\rho_{\min})$ ensures that either x_{N+1} is not the solution to Problem 7, or at least one σ_i^* exceeds ρ_{\min} . In both cases, $\eta_N^* \neq 0$ follows by the contrapositive of Lemma 12. \square

Consequently, we have the following continuity result:

Lemma 27 *Assumption 25 ensures that $v(t)$ is continuous over $(0, t_b]$.*

PROOF. Assumption 25 guarantees that, for each t , solutions exist for Problem 10. For each t , we select one solution and denote it as $z^*(t)$. Consequently, we can apply Theorem 8 to Problem 10 at the point $(z^*(t), t)$ for all t , with the prerequisites of Theorem 8 being met by Assumption 25 and Lemma 32 in the Appendix. The compactness in Theorem 8 is satisfied by the same method used in Lemma 34 in the Appendix. \square

Since $v(t)$ is a continuous function of t , we can apply the bisection search method to find the transition point. Under Assumption 25, $v(0) = m^* + t_{fl}(\rho_{\min})$, and $v(t_b) > m^* + t_{fl}(\rho_{\min})$, where m^* is the optimal value of Problem 7. We let $t_{\text{low}} = 0$ and $t_{\text{high}} = t_b$. In each iteration, we choose $t_{\text{mid}} = (t_{\text{low}} + t_{\text{high}})/2$. If $v(t_{\text{mid}}) > m^* + t_{fl}(\rho_{\min})$, we replace t_{high} with t_{mid} . Otherwise, we replace t_{low} with t_{mid} . The following theorem is a direct consequence of a standard bisection search method argument, the fact that $v(t)$ is continuous and Lemma 26.

Theorem 28 Under Assumption 25, for any $\epsilon > 0$, the bisection search method finds a $t_s^* \in (0, t_b)$ ensuring the following inequality within finite iterations:

$$m^* + t_f l(\rho_{\min}) < v(t_s^*) < m^* + t_f l(\rho_{\min}) + \frac{\epsilon}{2},$$

where m^* is the optimal value of Problem 7. Meanwhile, the Problem 9 generated by t_s^* is normal.

Remark 29 The complexity of the bisection search is logarithmic: given horizon T_f and precision Δt_{\min} , the maximum number of iterations is $N = \log_2(T_f/\Delta t_{\min})$. For example, $T_f = 10$ min and $\Delta t_{\min} = 1$ s yield $N \approx 10$. In practice, the computational burden is often lower than expected for several reasons: (i) long-horizon cases typically occur in early stages, where the problem size and complexity are lower; (ii) early termination is possible once a satisfactory solution is found; and (iii) warm-starting from previous solutions is available in the MPC framework.

Since the Problem 9 generated by t_s^* is normal, we can now add the perturbation and apply the results from Theorem 20 and 21. As tuning the switch point changes the horizon and discretization of Problem 9, we cannot directly compare the solution of Problem 9 to that of the discrete Problem 3. Therefore, we directly compare the result of Problem 9 to that of the continuous-time Problem 1. Note that the best possible solution for Problem 1 is the one with control $g(u(t)) = \rho_{\min}$ for all t and $m(x(t_f))$ equal to m^* , where m^* is the optimal value of Problem 7. The next theorem shows that the solution of Problem 9 with perturbation achieves $m(x(t_f))$ almost equal to m^* , and $g(u_i)$ less than ρ_{\min} up to an arbitrarily small $\epsilon > 0$.

To do this, we need a few notations consistent with those of Theorem 20. Consider the Problem 9 generated from t_s^* . We add a perturbation $q \in \mathbb{R}^d$ to the dynamics matrix $A(t_s^*)$ and denote the perturbed matrix as $\tilde{A}(t_s^*, q)$. The optimal solution of the resulting perturbed optimization problem is denoted as $(x(q), u(q), \sigma(q))$. If we plug in $u(q)$ into the original dynamics, we have

$$\begin{aligned} \tilde{x}_{N+1}(q) &= x_1 + \sum_{i=1}^N A(t_s^*)^{i-1} B(t_s^*) u_i(q) \\ &= x_1 + \sum_{i=1}^N \tilde{A}^{i-1}(t_s^*, 0) B(t_s^*) u_i(q) \end{aligned}$$

Here, $\tilde{x}_{N+1}(q)$ is denoted to be the endpoint of the propagated trajectory if we apply the control acquired from the perturbed problem to the original dynamics.

Theorem 30 Assume Assumption 25 is valid, Choose a function $l: \mathbb{R} \rightarrow \mathbb{R}$ for Problem 9 such that the derivative of l is larger than some $L_l > 0$ within the domain of σ . Then, for any $\epsilon > 0$, we can acquire $t_s^* \in \mathbb{R}$ and $\delta > 0$ such that for any perturbation $q \in \mathbb{R}^d$ with $\|q\| < \delta$ applied to Problem 9 generated by t_s^* , the control $u(q)$ and the propagated trajectory $\tilde{x}_{N+1}(q)$ satisfies:

- $\|G(\tilde{x}_{N+1}(q))\| \leq \delta$,

- $g(u_i) \geq \rho_{\min}$ for all i up to $n_x - 1$ points with probability one.
- $\rho_{\min} + \epsilon > g(u_i)$ for all i ,
- $m^* + \epsilon > m(\tilde{x}_{N+1}(q))$,

where m^* is the solution to Problem 7.

PROOF. See Appendix 8.6 \square

Theorem 30 guarantees the validity of adding perturbation to the dynamics. Consequently, we introduce Algorithm 1, which is capable of handling both normal and long-horizon cases. This algorithm provides a control sequence that at most violates the original nonconvex constraints at $n_x - 1$ grid points. In practical applications, the perturbation step is likely to remain deactivated since it serves primarily for theoretical completeness and is activated only in artificial edge cases.

6 Numerical Examples

In this section, we present three illustrative numerical examples. The first and third examples simulate Moon landing scenarios for the normal and long-horizon cases, respectively. The second example is an artificial case designed to demonstrate the necessity of perturbation and the tightness of the $n_x - 1$ bound in Theorem 20. All computations are performed using CVXPY [Diamond and Boyd \[2016\]](#).

One can verify that Assumptions 2, 3, 5, 6, and 14 hold for the first and second examples. However, directly testing Slater's Condition in Assumption 25 for the third example is challenging, as it requires verification for all $t_s \in [0, t_b]$. Developing a method to test this assumption is left for future research. All other conditions in Assumption 25 are satisfied for the third example.

6.1 Well-Conditioned Example

We consider a Moon landing problem where the objective is to guide the spacecraft from an initial state to a target state while satisfying thrust constraints. The state variable is a six-dimensional vector, where the first three components represent position and the last three components represent velocity. The spacecraft has a constant mass of $\bar{m} = 1000$ kg, an initial velocity of $(0, 3, -50)$ m/s, and an initial position of $(0, 0, 5000)$ m. The thrust is constrained between a minimum and a maximum value, where the maximum thrust T_{\max} is 7500 N, and the actual thrust range is $[0.3, 0.8]$ of the maximum thrust. The gravitational acceleration on the Moon is -1.62 m/s² in the z axes. The target state is a low-speed descent at $(0, 0, 100)$ m with velocity $(0, 0, -5)$ m/s, allowing a smooth transition to subsequent control phases. The values of these parameters are adjusted based on the data provided in [Sostaric and Rea \[2005\]](#).

This problem follows the same formulation as Problem 4, with the only difference being in the dynamics. The control variable represents the thrust-to-mass ratio. Since the final state is fixed, the terminal cost function $m(x_{N+1})$ is set to zero, and the fixed final state

Algorithm 1 LCvx Method with Bisection for the Long Horizon Cases

Require: $A_c, B_c, A, B, u_s, x_s, \rho_{\min}, \epsilon_t > 0, \epsilon_q > 0$

Ensure: Optimized time t_s , state x , control u , and slack variables σ

```

1: Set  $t_{\text{low}} = 0, t_{\text{high}} = t_f, t_s^* = 0, x_{\text{init}} = x_s$ 
2: Solve Problem 4 to obtain  $x, u, \sigma$ 
3: if  $\sigma_i > \rho_{\min}$  for some  $i$  or  $x_{N+1}$  doesn't solve Problem 7 then
4:   if the number of nodes that LCvx being invalid  $\leq n_x - 1$  then
5:     return  $t_s^*, x, u, \sigma$ 
6:   else
7:     Perturb the optimization Problem 4 with randomly generated  $\|q\| \leq \epsilon_q$ 
8:     Solve the perturbed Problem 4 to obtain  $x, u, \sigma$ 
9:   return  $t_s^*, x, u, \sigma$ 
10:  end if
11: end if
12: Modify the object function  $l_i$  to  $l(\sigma_i) \times (t_f - t_s)/N$  that satisfies assumption in Theorem 30
13: Set  $t_s = (t_{\text{low}} + t_{\text{high}})/2$ 
14: while  $(t_{\text{high}} - t_{\text{low}}) > \epsilon_t$  do
15:   Solve Problem 9 defined by  $t_s$  and  $u_s$  to obtain  $x, u, \sigma$ 
16:   if  $\sigma_i > \rho_{\min}$  for some  $i$  or  $x_{N+1}$  doesn't solve Problem 7 then
17:     Set  $t_{\text{low}}, t_{\text{high}} = t_{\text{low}}, t_s$ 
18:   else
19:     Set  $t_{\text{low}}, t_{\text{high}} = t_s, t_{\text{high}}$ 
20:   end if
21:    $t_s = (t_{\text{low}} + t_{\text{high}})/2$ 
22: end while
23:  $t_s^* = t_{\text{high}}$ 
24: Solve Problem 9 defined by  $t_s^*$  to obtain  $x, u, \sigma$ 
25: if the number of nodes that LCvx being invalid  $\leq n_x - 1$  then
26:   return  $t_s^*, x, u, \sigma$ 
27: else
28:   Perturb the optimization Problem 9 by  $\|q\| \leq \epsilon_q$  to obtain  $x, u, \sigma$ 
29:   return  $t_s^*, x, u, \sigma$ 
30: end if

```

constraint is enforced through $G(x_{N+1}) = 0$. The cost function $l(\sigma)$ is defined as the absolute value, minimizing control effort. The thrust constraints are given by $\rho_{\min} = 0.3T_{\max}/\bar{m}$ and $\rho_{\max} = 0.8T_{\max}/\bar{m}$, with a total flight time of $t_f = 60$ s.

The key difference from Problem 4 is the inclusion of lunar gravity. The discrete-time dynamics are given by

$$x_{i+1} = Ax_i + B(u_i + g),$$

where $g = (0, 0, -1.62)$ represents lunar gravity. The matrices A and B are obtained from the continuous-time

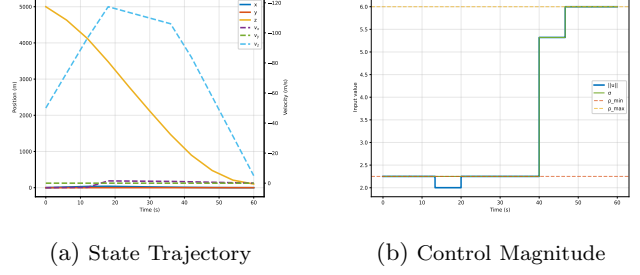


Fig. 1. State trajectory and control magnitude for the Moon landing problem over a 60-second flight. (a) Position and velocity evolution, with velocity plotted on an inverted axis. (b) Control norm, thrust bounds, and σ evolution. One LCvx invalid point occurs where the control norm falls below ρ_{\min} .

dynamics:

$$A_c = \begin{bmatrix} 0_{2 \times 2} & I_{2 \times 2} \\ 0_{2 \times 2} & 0_{2 \times 2} \end{bmatrix}, \quad B_c = \begin{bmatrix} 0_{2 \times 2} \\ I_{2 \times 2} \end{bmatrix},$$

and discretized using N time steps via Equation (1). Compared to Problem 4, the dynamics include an additional perturbation term due to gravity, which does not affect the theoretical discussions in the previous section.

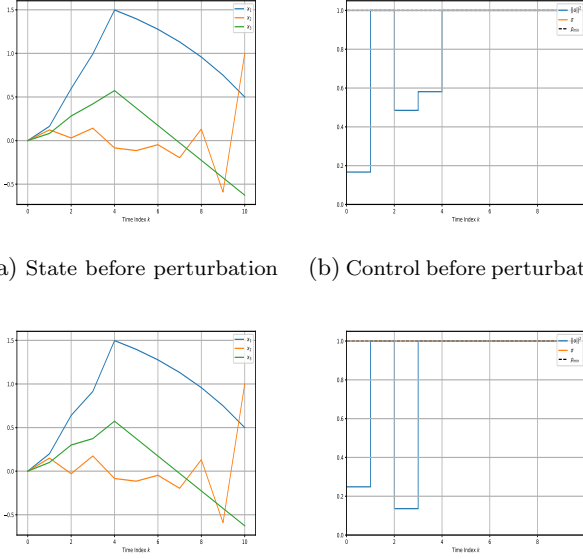
The solution trajectory and control magnitudes for $N = 10$ are shown in Figure 1. We observe that LCvx is invalid at one temporal grid, indicating that the solution to Problem 4 does not always satisfy the constraints of Problem 3, even for a well-conditioned problem. Additionally, we tested the extent of LCvx violations under finer discretizations. With $N = 30, 50, 100, 300$, we observed one violation for $N = 50$ and 500, and no violations for $N = 30$ and 300. This confirms that the number of violations does not depend on the discretization level, consistent with our theoretical results.

6.2 Artificial normal example

In this section, we consider a three-dimensional problem with $N = 10$, $A = \text{diag}(1.2, -2.2, 1)$, and $B = (0.4, 0.3, 0.2)^\top$. Notice that A and B forms a controllable matrix pair.

$$\begin{aligned}
& \min_{x, u, \sigma} \quad x_{11,3} + \sum_{i=1}^{10} \sigma_i \\
& \text{s. t.} \quad x_{i+1} = Ax_i + Bu_i, \quad i \in [1, 10]_{\mathbb{N}} \\
& \quad x_1 = [0, 0, 0]^\top, \quad x_{11,1} = 0.5, \quad x_{11,2} = 1 \\
& \quad 1 \leq \sigma_i \leq 2, \quad \|u_i\|^2 \leq \sigma_i, \quad i \in [1, 10]_{\mathbb{N}}
\end{aligned}$$

Here, the dynamics do not come from any continuous system, as A has negative eigenvalues. This counterexample is formed by making the matrix Λ in the proof of Theorem 20 singular. The numerical tolerance for CVXPY is set to 10^{-12} . The solution trajectory is available in Figure 2a, and the magnitude of the control is shown in Figure 2b. We observe that LCvx is invalid at three points. According to Theorem 20, adding a perturbation to the dynamics reduces the violation of non-convex constraints to at most two points. We consider



(a) State before perturbation (b) Control before perturbation
(c) State after perturbation (d) Control after perturbation

Fig. 2. System dynamics and control response before and after perturbation for an artificial three-dimensional problem with $N = 10$ temporal grid points. The top figures display the state trajectory and control magnitude prior to perturbation, revealing LCvx invalid at three points. The bottom figures show the system's response to a perturbation designed as per Theorem 20, which reduces the number of nonconvex constraint violations to two. The state variable remains essentially unchanged.

the following dynamics with $A_p = \text{diag}(10^{-7}, 0, 0)$:

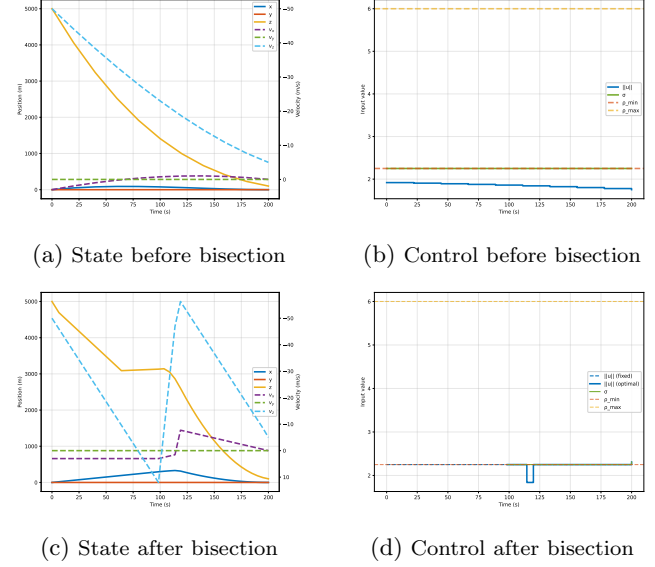
$$x_{i+1} = (A + A_p)x_i + Bu_i, \quad i \in [1, 10]_{\mathbb{N}}$$

which introduces a small change to one element in the dynamics matrix. The updated trajectory and control sequence are available in Figure 2c and Figure 2d, respectively. As expected, LCvx is invalid at two points after perturbation.

6.3 Long-horizon example

Our final example is a long-horizon case that follows the same setup as our first example, with the distinction that we have $N = 20$ and $t_f = 200$. The trajectory and control magnitude are presented in Figures 3a and 3b. These figures show that all control magnitudes are less than $\rho_{\min} = 1$, confirming that this is indeed a long-horizon case.

Next, we apply the bisection search method described in Algorithm 1, setting $\epsilon_t = 10^{-2}$ and initializing the control as $[0, 0, \rho_{\min}]^T$. The algorithm terminates with $t_s = 98.4$ after seven bisection steps. This suggests maintaining the initial control for 98.4 seconds before switching to a control sequence generated by Problem 9. The resulting trajectory and control magnitude are shown in Figures 3c and 3d. The control magnitude plot reveals one LCvx invalidation.



(a) State before bisection (b) Control before bisection
(c) State after bisection (d) Control after bisection

Fig. 3. State trajectory and control magnitude for the Moon landing problem over a 200-second flight. (a,c) Position and velocity evolution before and after the bisection search, with velocity plotted on an inverted axis. (b,d) Control norm, thrust bounds, and σ evolution before and after the bisection search. Figures (a,b) indicate a long-horizon state where the control magnitudes remain below the threshold ρ_{\min} . Figures (c,d) demonstrate the effectiveness of the bisection search method described in Algorithm 1, resulting in a trajectory that exhibits an LCvx violation at one point. The information for σ is not available before the transition point.

7 Conclusion

In this paper, we develop a new theoretical framework for the application of Lossless Convexification (LCvx) to discrete-time nonconvex optimal control problems, addressing a gap in the existing LCvx literature. Specifically, we establish theoretical guarantees that, under mild assumptions, the optimal solution of the relaxed convex problem satisfies the constraints of the original nonconvex problem at all but at most $n_x - 1$ temporal grid points when an arbitrarily small perturbation is introduced into the dynamic constraints, where n_x is the state dimension. Furthermore, we analyze the limitations of the existing LCvx method in long-horizon cases where the transversality condition does not hold and demonstrate how our framework can be extended to handle these cases via a bisection-based approach. Numerical examples illustrate the necessity of the perturbation, the tightness of the $n_x - 1$ upper bound, and the practical applicability of our theoretical framework to long-horizon problems.

For future work, we aim to investigate the theoretical guarantees of applying the LCvx method to various forms of discrete-time nonconvex optimal control problems. Furthermore, we plan to extend our results to develop a lossless convexification method that ensures continuous-time constraint satisfaction [Elango et al., 2024].

8 Appendix

8.1 Proof of theorem 8

PROOF. Let y^* be the optimal solution to Problem 6 at p_0 , satisfying assumptions in Lemma 7. The existence of y^* is a consequence of the compactness of Ω and the continuity of the object function. Lemma 7 ensures the existence of $\delta > 0$ and $\xi > 0$ such that for any $p \in \mathbb{R}^{n_p}$ with $|p - p_0| < \xi$, there is a point $y \in \Omega$, $F(y, p) = 0$ and

$$\|y - y^*\| \leq \frac{\|F(y^*, p)\|}{\delta}.$$

Hence, the feasible set for Problem 6 is nonempty for p sufficiently close to p_0 . Additionally, because Ω is a compact set, optimal solutions exist for Problem 6 for p sufficiently close to p_0 .

We first prove that $\liminf_{s \rightarrow p_0} M^*(s) \geq M^*(p_0)$. Consider a sequence $s_k \in \mathbb{R}^{n_p}$ sufficiently close to p_0 such that $\lim_k M^*(s_k) = \liminf_{s \rightarrow p_0} M^*(s)$ and $\lim_k s_k = p_0$. We denote the optimal solution of the Problem 6 generated by s_k as y_k . Due to the compactness of Ω , there exist a convergent subsequence y_{k_n} and a variable \bar{y} such that $\lim_n y_{k_n} = \bar{y}$ and $\liminf_{s \rightarrow p_0} M^*(s) = \lim_n M^*(s_{k_n}) = \lim_n M(y_{k_n}, s_{k_n})$. Due to the continuity of $F(y, p)$ and the closedness of Ω , \bar{y} is feasible for Problem 6 generated by p_0 . Thus, $\lim_n M^*(s_{k_n}) = \lim_n M(y_{k_n}, s_{k_n}) = M(\bar{y}, p_0) \geq M^*(p_0)$ by the continuity of $M(\cdot, \cdot)$.

Next, we aim to show that $\limsup_{w \rightarrow p_0} M^*(w) \leq M^*(p_0)$. As the object function $M(y, p)$ is locally Lipschitz and y lies in a compact set, there exists a Lipschitz constant L_M for all feasible (y, p) when $\|p - p_0\| < \xi$.

Consider a sequence w_k such that $\lim_k M^*(w_k) = \limsup_{w \rightarrow p_0} M^*(w)$ with $|w_k - p_0| < \xi$ and $\lim_k w_k = p_0$. Lemma 7 ensures the existence of a corresponding sequence $y_k \in \Omega$ that $F(y_k, w_k) = 0$,

$$\|y_k - y^*\| \leq \frac{\|F(y^*, w_k)\|}{\delta},$$

and $M^*(w_k) \leq M(y_k, w_k)$. Therefore,

$$\begin{aligned} \limsup_{w \rightarrow p_0} M^*(w) &= \lim_k M^*(w_k) \\ &\leq \limsup_k M(y_k, w_k) \\ &\leq \limsup_k (M(y^*, w_k) + L_M \|y_k - y^*\|) \quad (6) \\ &\leq M(y^*, p_0) + L_M \limsup_k \frac{\|F(y^*, w_k)\|}{\delta} \\ &= M(y^*, p_0) + \frac{\|F(y^*, p_0)\|}{\delta} = M^*(p_0). \quad (7) \end{aligned}$$

Here, inequality (6) is due to the Lipschitz property of M and inequality (7) is due to the continuity of F .

In summary, we have

$$\limsup_{p \rightarrow p_0} M^*(p) \leq M^*(p_0) \leq \liminf_{p \rightarrow p_0} M^*(p),$$

thus establishing the continuity of M^* . \square

8.2 Proof for Lemma 17

Since Assumption 2 trivially holds, we start by showing the validity of Assumptions 3 and 5.

Lemma 31 *Suppose that Assumptions 3 and 5 hold for Problem 8 at $q = 0$. Then, there exists an $\epsilon > 0$ such that for any $q \in \mathbb{R}^d$ within the cube $\epsilon\mathbb{D} \in \mathbb{R}^d$, where $\mathbb{D} \subset \mathbb{R}^d$ is a unit cube, both assumptions are satisfied for Problem 8 generated by q .*

PROOF. The proof of both assumptions relies on the fact that the determinant of a matrix is a continuous function of elements in that matrix. We demonstrate Assumption 3 for Problem 8, while the nonsingularity of $\nabla_z H$ in Assumption 5 follows similarly and thus is omitted.

Define

$$S(q) := \begin{pmatrix} B & \tilde{A}(q)B & \dots & \tilde{A}(q)^{n_x-1}B \end{pmatrix}.$$

We aim to show that $S(q)$ retains full rank for all q within $\epsilon\mathbb{D}$. $S(q)$ has full rank if and only if the determinant of $S(q)S(q)^\top$ is nonzero. As the elements in matrix \tilde{A} are continuous functions of q , the elements and, consequently, the determinant of $S(q)S(q)^\top$ are continuous functions of q . Given that $\tilde{A}(0) = A$, the controllability of the matrix pair $\{A, B\}$ ensures that $S(0)$ has full rank and that the determinant of $S(0)S(0)^\top$ is nonzero. Through continuity, an $\epsilon > 0$ exists such that for any q within $\epsilon\mathbb{D}$, the determinant of $S(q)S(q)^\top$ remains nonzero, and $S(q)$ maintains full rank. \square

Now, we turn to prove that Assumption 6 holds after perturbation. To simplify the notation for Problem 8, we let $z = (x, u, \sigma)$. The object function $\Phi(z)$ and the set \tilde{V} formed by inequalities are the same as in Problem 5. The affine constraint function $H(z)$ in Problem 5 is augmented to $\tilde{H}(z, q)$ to accommodate the dynamics and boundary constraints of Problem 8. Thus, our perturbed problem can be represented as:

$$\begin{aligned} \min_z \quad & \Phi(z) \\ \text{s.t.} \quad & \tilde{H}(z, q) = 0, \quad z \in \tilde{V}, \end{aligned}$$

When $q = 0$, we have $\tilde{H}(z, 0) = H(z)$, thereby retrieving the original Problem 5.

Since we need lemma 7 and theorem 8 for our discussion, we must demonstrate that their assumptions are valid.

Lemma 32 *Assumption 5 and Assumption 6 for Problem 4 ensures that for any vector z_0 such that*

$$\tilde{H}(z_0, 0) = 0, \quad z_0 \in \tilde{V},$$

we have that $y = 0$ is the unique solution of the following equation:

$$0 \in \nabla_z \tilde{H}(z_0, 0)^\top y + N_{\tilde{V}}(z_0)$$

PROOF. We prove this statement by contradiction. Assume there exists $y \neq 0$ such that

$$0 \in \nabla_z \tilde{H}(z_0, 0)^\top y + N_{\tilde{V}}(z_0).$$

Consider the function $g(z) = y^\top \tilde{H}(z, 0) + I_{\tilde{V}}(z)$, where $I_{\tilde{V}}(z)$ is the indicator function for the set \tilde{V} . Thus we have $0 \in \partial g(z_0)$ and $\tilde{H}(z_0, 0) = 0$. Since $g(z)$ is a convex function, the minimum of $g(z)$ is zero, achieved at z_0 .

Given Assumption 6, there exists an interior point z' in \tilde{V} where $\tilde{H}(z', 0) = 0$ and $N_{\tilde{V}}(z') = \{0\}$. Therefore, z' is also a minimizer of the function g , and thus $0 \in \partial g(z') = y^\top \nabla_z \tilde{H}(z', 0)$. Meanwhile, $\nabla_z \tilde{H}(z', 0) = \nabla_z \tilde{H}(z_0, 0)$ because H is an affine function of variable z . Consequently, the vector y lies in the left null space of $\nabla_z \tilde{H}(z, 0)$, which contradicts Assumption 5. \square

Now, we are ready to prove that Assumption 6 holds after perturbation:

Lemma 33 *Suppose that Assumption 5 and 6 hold for Problem 8 when $q = 0$. Then, there exists an $\epsilon > 0$ such that for any $q \in \mathbb{R}^d$ within the cube $\epsilon\mathbb{D} \in \mathbb{R}^d$, where $\mathbb{D} \in \mathbb{R}^d$ is an unit cube, such that the perturbed Problem 8 with respect to q also satisfies Assumption 6.*

PROOF. Slater's assumption implies the existence of a z_0 such that $H(z_0) = \tilde{H}(z_0, 0) = 0$, while z_0 lies in the interior of \tilde{V} . Since Lemma 32 ensures the applicability of Lemma 7, there exist $\epsilon_1 > 0$ and $\delta > 0$ such that for all $\|q\| < \epsilon_1$, there exists a $z(q)$, determined by q , satisfying

$$\|z(q) - z_0\| \leq \frac{\|\tilde{H}(z_0, q)\|}{\delta},$$

and $\tilde{H}(z(q), q) = 0$, thus meeting the dynamics and boundary conditions of Problem 8. Given that \tilde{H} is a continuous function, there exists an $\epsilon > 0$, such that when $\|q\| < \epsilon$, $\|z(q) - z_0\|$ is sufficiently small for $z(q)$ to lie in the interior of \tilde{V} , thereby validating Slater's condition for the perturbed problem. \square

Now we show that the perturbed problem is normal.

Lemma 34 *Suppose that Assumptions 2, 5, 6 and 14 hold for Problem 8 and $q = 0$. Then there exists an $\epsilon > 0$ such that for any q within the cube $\epsilon\mathbb{D}$, Assumption 14 is still valid for Problem 8 after perturbation by q .*

PROOF. We apply Theorem 8 to show that the optimum value of Problem 8 is continuous with respect to q . To satisfy the theorem's assumptions, we introduce a sufficiently large trivial upper bound on σ , ensuring the compactness of \tilde{V} . Assumption 2 guarantees that the optimal solution remains unchanged with or without this upper bound. Consequently, Assumption 2 and Lemma 32 confirm the validity of assumptions to Theorem 8.

Since when $q = 0$ Problem 4 is normal, the optimal value of Problem 4 is larger than $m^* + \sum_{i=1}^N l_i(\rho_{\min})$, where m^* is the minimum value of Problem 7. Thus,

the continuity of the optimal value function ensures the existence of an $\epsilon > 0$ such that for all $q \in \epsilon\mathbb{D}$, the optimal value of Problem 8 generated by $\{\tilde{A}(q), B\}$ is greater than $m^* + \sum_{i=1}^N l_i(\rho_{\min})$. Assumption 2 ensures that l_i are monotone, indicating that the perturbed problem is still normal. \square

8.3 Proof for Theorem 20

The following is a useful linear algebra theorem from [Chen, 1984, Theorem 3.5] that aids us in proving Theorem 20.

Theorem 35 *Consider a function $f(\lambda)$ and a matrix $A \in \mathbb{R}^{n \times n}$. The characteristic polynomial of A is*

$$\Delta(\lambda) = \det(I - \lambda A) = \prod_{i=1}^d (\lambda - \lambda_i)^{m_i},$$

where m_i are the algebraic multiplicity of eigenvalue λ_i , $n = \sum_{i=1}^d m_i$, and d is the total number of distinct eigenvalues.

There exists a polynomial $h(\lambda)$ as

$$h(\lambda) := v_0 + v_1 \lambda + \dots + v_{n-1} \lambda^{n-1}, \quad (8)$$

such that

$$f(A) = h(A).$$

The unknown coefficients of (8) are found by solving n equations:

$$f^{(l)}(\lambda_i) = h^{(l)}(\lambda_i) \text{ for } l \in [0, m_i - 1]_{\mathbb{N}}, i \in [1, d]_{\mathbb{N}}, \quad (9)$$

where

$$f^{(l)}(\lambda_i) := \left. \frac{d^l f(\lambda)}{d\lambda^l} \right|_{\lambda=\lambda_i},$$

and $h^{(l)}(\lambda_i)$ is defined in the same manner.

Now we start the proof for 20.

PROOF. [Proof for Theorem 20] If $n_x > N$, the statement holds trivially; thus, we assume $n_x \leq N$. We choose $\epsilon > 0$ sufficiently small that Lemma 17 is valid. Thus, the perturbed Problem 8 has controllable dynamics, is normal, and satisfies Slater's condition.

Consider the matrix

$$S(q) := \begin{pmatrix} \tilde{A}(q)^{P_1} B & \tilde{A}(q)^{P_2} B & \dots & \tilde{A}(q)^{P_{n_x}} B \end{pmatrix},$$

for specific integers $1 \leq P_1 < P_2 < \dots < P_{n_x} < N + 1$, where N is the total number of grid points in Problem 8, $\tilde{A}(q)$ is the perturbation of A with respect to q and n_x is the state dimension.

According to Lemma 19, if $S(q)$ is of full rank, then the Problem 8 generated by $\{\tilde{A}(q), B\}$ satisfies LCvx at least at one point among the set $\{N - P_1, N - P_2, \dots, N - P_{n_x}\}$.

We aim to demonstrate that $S(q)$ is of full rank with probability one, regardless of the choice of P_1 to P_{n_x} .

According to Theorem 35, all powers of the matrix $\tilde{A}(q)$ can be written as polynomials of $\tilde{A}(q)$ up to the

power $n_x - 1$. Then, there exists a matrix $V(q) \in \mathbb{R}^{n_x \times n_x}$ such that

$$\tilde{A}^{P_i}(q) = \sum_{j=1}^{n_x} V_{ij}(q) \tilde{A}^{j-1}(q), \quad i \in [1, n_x]_{\mathbb{N}}$$

Here, V_{ij} represents the element in the i -th row and j -th column of $V(q)$.

Now we show that $V(q)$ being invertible is sufficient for $S(q)$ to be of full rank: Let $W(q)$ be the inverse of $V(q)$, Then

$$\tilde{A}^i(q) = \sum_{j=1}^{n_x} W_{ij}(q) \tilde{A}^{P_i}(q), \quad i \in [1, n_x]_{\mathbb{N}} \quad (10)$$

If $S(q)$ has a nonzero left null vector ξ , we have $\xi \tilde{A}^{P_i}(q) B = 0$ for all $i \in [1, n_x]_{\mathbb{N}}$. Equation (10) implies that $\xi \tilde{A}^i(q) B = 0$, for all $i \in [0, n_x - 1]_{\mathbb{N}}$ contradicting controllability ensured by Lemma 17.

Therefore, $V(q)$ being invertible is sufficient for $S(q)$ to be of full rank. We thus have

$\text{Prob}(\text{rank}(S(q)) < n_x) \leq \text{Prob}(V(q) \text{ being singular})$
The rest of this proof is to show that the probability on the right-hand side is zero.

Setting the distinct eigenvalues of A as $\lambda_1, \lambda_2, \dots, \lambda_d$, the eigenvalues of the perturbed matrix $\tilde{A}(q)$ have eigenvalues $\tilde{\lambda}_i = \lambda_i + q_i$ for $i \in \{1, 2, \dots, d\}$. Here, d is the number of distinct eigenvalues of A .

We start by exploring how $V(q)$ is determined by the eigenvalues $\tilde{\lambda}_i = \lambda_i + q_i$. The characteristic polynomial of A can be written as: $\prod_{i=1}^d (\lambda - \lambda_i)^{m_i}$ where $\sum_{i=1}^d m_i = n_x$ with m_i being the algebraic multiplicity of λ_i .

Due to the perturbation preserving the Jordan form, the characteristic polynomial of \tilde{A} becomes:

$$\prod_{i=1}^d (\lambda - \tilde{\lambda}_i)^{m_i} = \prod_{i=1}^d (\lambda - \lambda_i - q_i)^{m_i},$$

where $\sum_{i=1}^d m_i = n_x$. It is clear that the probability of

$$\tilde{\lambda}_i = \lambda_i + q_i = \lambda_j + q_j = \tilde{\lambda}_j$$

holding for any i and j is zero. Consequently, we retain d distinct eigenvalues with probability one.

According to Theorem 35, $V(q)$ consists of the coefficients in (8) for each P_i . For the P_i power of $\tilde{A}(q)$ and an eigenvalue $\tilde{\lambda}_j$, the equation (9) for the i -th row of $V(q)$ is:

$$\begin{aligned} \tilde{\lambda}_j^{P_i} &= V_{i1} + V_{i2} \tilde{\lambda}_j + \dots + V_{in_x} \tilde{\lambda}_j^{n_x-1}, \\ P_i \tilde{\lambda}_j^{P_i-1} &= 0 + V_{i2} + \dots + V_{in_x} (n_x - 1) \tilde{\lambda}_j^{n_x-2}, \\ &\vdots \\ \prod_{k=0}^{m_j-2} (P_i - k) \tilde{\lambda}_j^{P_i-m_j+1} &= \end{aligned}$$

$$0 + \dots + V_{in_x} \prod_{k=1}^{m_j-1} (n_x - k) \tilde{\lambda}_j^{n_x-m_j}.$$

Combining all equations for different P_i and $\tilde{\lambda}_j$, there are in total n_x^2 unknown variables in $V(q)$ and n_x^2 equations. We now write all equations into a matrix equality.

For the P_i -th power and the j -th eigenvalue, to simplify the notation, we define Λ_{ij} as

$$\left[\tilde{\lambda}_j^{P_i}, P_i \tilde{\lambda}_j^{P_i-1}, \dots, \prod_{k=0}^{m_j-2} (P_i - k) \tilde{\lambda}_j^{P_i-m_j+1} \right],$$

T_j as

$$\begin{bmatrix} 1 & 0 & \dots & 0 \\ \tilde{\lambda}_j & 1 & \dots & 0 \\ \tilde{\lambda}_j^2 & 2\tilde{\lambda}_j & \dots & 0 \\ \vdots & \vdots & \ddots & \vdots \\ \tilde{\lambda}_j^{n_x-1} & (n_x - 1) \tilde{\lambda}_j^{n_x-2} & \dots & \prod_{k=1}^{m_j-1} (n_x - k) \tilde{\lambda}_j^{n_x-m_j} \end{bmatrix},$$

and

$$V_i = [V_{i1}, V_{i2}, \dots, V_{in_x}].$$

Thus, we have $\Lambda_{ij} = V_i T_j$. Stacking Λ and T into matrices, we have

$$\Lambda = \begin{bmatrix} \Lambda_{11} & \Lambda_{12} & \dots & \Lambda_{1d} \\ \vdots & \vdots & \ddots & \vdots \\ \Lambda_{n_x 1} & \Lambda_{n_x 2} & \dots & \Lambda_{n_x d} \end{bmatrix}$$

and

$$T = [T_1, T_2, \dots, T_d].$$

According to Theorem 35, the matrix $V(q)$ must satisfy

$$\Lambda = VT,$$

where Λ , V , and T are n_x -by- n_x matrices and functions of q . The determinant of Λ is the product of the determinants of V and T . Hence, for V to be singular, Λ must also be singular.

We establish the non-singularity of Λ through induction. To begin, we construct a sequence of matrices $C_k \in \mathbb{R}^{M_k \times M_k}$, for $k = 1, 2, \dots, d$ and $M_k = \sum_{i=1}^k m_i$. Each C_k is designed to be a square matrix formed from the top-left corner of the matrix Λ . Specifically C_k is defined as:

$$C_k = \begin{bmatrix} \Lambda_{11} & \dots & \Lambda_{1k} \\ \vdots & & \vdots \\ \Lambda_{M_k 1} & \dots & \Lambda_{M_k k} \end{bmatrix}_{M_k \times M_k}.$$

As $n_x = \sum_{i=1}^d m_i$, where d is the number of distinct eigenvalues that A has, it follows that $C_d = \Lambda$.

We initiate induction by proving that the probability of C_1 being singular is zero. Substituting the expression of Λ_{ij} into the definition of C_1 , we obtain:

$$C_1 = [\Lambda_{11}^\top, \Lambda_{21}^\top, \dots, \Lambda_{M_1 1}^\top]^\top = \begin{bmatrix} \tilde{\lambda}_1^{P_1} & P_1 \tilde{\lambda}_1^{P_1-1} \dots & \prod_{r=0}^{m_1-2} (P_1 - r) \tilde{\lambda}_1^{P_1-m_1+1} \\ \vdots & \vdots & \vdots \\ \tilde{\lambda}_1^{P_{m_1}} & P_{m_1} \tilde{\lambda}_1^{P_{m_1}-1} \dots & \prod_{r=0}^{m_1-2} (P_{m_1} - r) \tilde{\lambda}_1^{P_{m_1}-m_1+1} \end{bmatrix}.$$

The determinant of C_1 is computed as a sum of signed products of matrix entries. Each summand in this sum represents a product of distinct entries, with no two entries sharing the same row or column. Consequently, all summands contribute to the same power order of $\tilde{\lambda}_1$. Therefore, the determinant of C_1 can be expressed as:

$$\det(C_1) = c_1 \tilde{\lambda}_1^{\sum_{r=1}^{m_1} P_r - \sum_{r=1}^{m_1} (r-1)},$$

with constant c_1 .

The expression for c_1 can be found by setting $\tilde{\lambda}_1 = 1$, as this expression of C_1 holds for all realizations of $\tilde{\lambda}_1$. We denote E_1 as the matrix that generates c_1 , that is, $c_1 = \det(E_1)$. Each element in E_1 is a polynomial in P_i , where $i \in \{1, 2, \dots, m_1\}$. Notably, the polynomials in the same column share the same coefficients. This structure allows E_1 to be transformed into a Vandermonde matrix through column transformations. Given that P_i are distinct, this Vandermonde matrix is nonsingular, implying $c_1 \neq 0$. Thus C_1 is nonsingular as long as $\tilde{\lambda}_1 \neq 0$. Given that $\tilde{\lambda}_1$ follows a uniform distribution, the probability of $\tilde{\lambda}_1 = 0$ is zero. Therefore, C_1 is nonsingular with probability one.

Now, assuming that C_k is nonsingular with probability one, we show that C_{k+1} is also nonsingular with probability one. We start by showing that with fixed values of $\tilde{\lambda}_1, \tilde{\lambda}_2, \dots, \tilde{\lambda}_k$ and the condition that C_k being nonsingular, the conditional probability of C_{k+1} being nonsingular is one. Partition C_{k+1} into the following blocks:

$$\begin{bmatrix} C_k & D_{k+1} \\ R_{k+1} & S_{k+1} \end{bmatrix}.$$

Here, $R_{k+1} \in \mathbb{R}^{m_{k+1} \times M_k}$ does not contain $\tilde{\lambda}_{k+1}$, and $D_{k+1} \in \mathbb{R}^{m_{k+1} \times M_k}$ contains terms involving $\tilde{\lambda}_{k+1}$ up to order P_{M_k} . The terms of $\tilde{\lambda}_{k+1}$ with power higher than P_{M_k} are all included in $S_{k+1} \in \mathbb{R}^{m_{k+1} \times m_{k+1}}$.

Given the fixed values of $\tilde{\lambda}_1, \tilde{\lambda}_2, \dots, \tilde{\lambda}_k$, the determinant $\det(C_{k+1})$ becomes a polynomial in $\tilde{\lambda}_{k+1}$ with fixed coefficients. The term with the highest power in this polynomial arises from the product of elements in C_k with elements in S_{k+1} . The absolute value of the highest power term is in fact $|\det(C_k) \det(S_{k+1})|$.

Note that the matrix S_{k+1} shares the same pattern as C_1 . Following a similar line of reasoning as in the case of E_1 , we can conclude that the coefficient of $\det(S_{k+1})$ is also nonzero. Since C_k is nonsingular, the determinant

$\det(C_{k+1})$ has a nonzero leading term, implying that it has a finite number of roots. Meanwhile, the distribution of $\tilde{\lambda}_{k+1}$ is a uniform distribution independent of previous eigenvalues. Therefore, the conditional probability of $\tilde{\lambda}_{k+1}$ coinciding with these roots i.e.

$$\text{Prob}(C_{k+1} \text{ singular} | C_k \text{ nonsingular}, (\tilde{\lambda}_1, \dots, \tilde{\lambda}_k) \text{ fixed})$$

is zero. Note that $\text{Prob}(\tilde{\lambda}_1, \tilde{\lambda}_2, \dots, \tilde{\lambda}_k | C_k \text{ nonsingular})$ is a uniform distribution over the domain of $\tilde{\lambda}_1, \tilde{\lambda}_2, \dots, \tilde{\lambda}_k$, which is the set $\epsilon\mathbb{D}$ projected to the first k dimensional minus a measure zero set representing perturbations that make C_k singular. By integrating into $\tilde{\lambda}_1, \tilde{\lambda}_2, \dots, \tilde{\lambda}_k$, we deduce that:

$$\text{Prob}(C_{k+1} \text{ singular} | C_k \text{ nonsingular}) = 0.$$

Thus $\text{Prob}(C_{k+1} \text{ singular}) = 0$, as c_k is nonsingular with probability one.

Using induction, $\Lambda = C_d$ is nonsingular with probability one, which implies that V is also nonsingular. Consequently, $S(q)$ has full rank with probability one. Due to the discussion at the start of this proof, the probability of LCvx being invalid at all grid points $(N - P_1, N - P_2, \dots, N - P_{n_x})$ is zero. This means that, for any selection of n_x grid points, the probability of simultaneously violating the original nonconvex constraints at these points is zero. Hence, the probability of at least n_x violations of the original nonconvex constraints is also zero. \square

8.4 Proof for Theorem 21

PROOF. Since $\tilde{A}^i(\cdot)$ is a smooth function of the perturbation and the matrix norm is a Lipschitz function, there exists an ϵ_1 such that $\|\tilde{A}^i(\cdot)\|$ is a Lipschitz function for perturbations $\|q\| \leq \epsilon_1$ and for $i = 0, 1, 2, \dots, N-1$. Let L_A denote the maximum Lipschitz constant among all i of $\|\tilde{A}^i(\cdot)\|$. Additionally, Assumption 2 ensures that $u_i(q)$ is bounded, i.e., $\max \|u_i(q)\| < D$ for some $D > 0$. Therefore, when $\|q\| \leq \epsilon_1$, we can compare $\tilde{x}_{N+1}(q)$ with $x_{N+1}(q)$, and obtain:

$$\begin{aligned} & \|\tilde{x}_{N+1}(q) - x_{N+1}(q)\| \\ &= \left\| \sum_{i=1}^N (\tilde{A}^{i-1}(0) - \tilde{A}^{i-1}(q)) B u_i(q) \right\| \\ &\leq \sum_{i=1}^N L_A \|q\| \|B\| \|u_i(q)\| \leq N D L_A \|B\| \|q\|. \end{aligned}$$

Hence, $\tilde{x}_{N+1}(q)$ locates in a local neighborhood of $x_{N+1}(q)$ with radius $N D L_A \|B\| \epsilon_1$. Meanwhile, since G is an affine function and $G(x_{N+1}(0)) = 0$, we have $\|G(\tilde{x}_{N+1}(q))\| < \delta$, for sufficiently small $\|q\|$.

Now we move on to the second result. Since the control is bounded, $x(q)$ is bounded. Thus, $m(\cdot)$ in Problem 8 is a Lipschitz function within the domain of x because m is C^1 smooth. with Lipschitz constant L_m .

Thus:

$$|m(\tilde{x}_{N+1}(q)) - m(x_{N+1}(q))| \leq NDL_AL_m\|B\|\|q\|.$$

Meanwhile, Lemma 32, Lemma 34 (for the compactness), and Theorem 8 indicate that the optimum value of Problem 8 is continuous with respect to q . Therefore, for any $\delta > 0$ there exists $\epsilon > 0$ such that for all $\|q\| < \epsilon$,

$$\begin{aligned} m(\tilde{x}_{N+1}(q)) &+ \sum_{i=1}^N l_i(g(u_i(q))) \\ &\leq m(x_{N+1}(q)) + \sum_{i=1}^N l_i(g(u_i(q))) + K_q\|q\| \\ &\leq m(x_{N+1}(0)) + \sum_{i=1}^N l_i(g(u_i(0))) + K_q\|q\| + \delta/2 \\ &\leq m_o^* + K_q\|q\| + \delta/2, \end{aligned}$$

where $K_q = NDL_AL_m\|B\|$. Here, the second inequality arises from Theorem 8 that the optimum value of Problem 8 is continuous with respect to q , and that $(u(0), x_{N+1}(0))$ is the solution to the unperturbed problem. The last inequality is derived from the fact that the optimum value of Problem 4 lower bounds that of Problem 3. Hence, for sufficiently small $\|q\|$, we have $m(\tilde{x}_{N+1}(q)) + \sum_{i=1}^N l_i(g(u_i(q))) \leq m_o^* + \delta$. \square

8.5 Proof for Theorem 23

PROOF. Expanding the dynamics recursion yields

$$\|\hat{x}_{N+1} - x_{N+1}\| \leq \sum_{i=1}^N \|A^{N-i}B(\hat{u}_i - u_i)\|.$$

Using the relationship between A and A_c with the bound $\|exp(A_c t)\| \leq exp(\|A_c\|t)$, we have

$$\begin{aligned} &\|A^{N-i}B(\hat{u}_i - u_i)\| \\ &\leq e^{\|A_c\|t_f} \|B_c\| \|\hat{u}_i - u_i\| \int_0^{t_f/N} e^{\|A_c\|\tau} d\tau \\ &\leq e^{\|A_c\|t_f} \frac{\|B_c\|}{\|A_c\|} \rho_{\min}(e^{\|A_c\|t_f/N} - 1). \end{aligned}$$

Summing over at most $n_x - 1$ violations gives the first bound.

For asymptotically stable A_c , using the additional bound $\|exp(A_c t)\| \leq \beta(A_c)exp(-\alpha t)$ for some α and β depending on A_c [Bernstein, 2018, Fact 15.16.9], we obtain

$$\|A^{N-i}B(\hat{u}_i - u_i)\| \leq e^{\|A_c\|t_f} \|B_c\| \rho_{\min} \beta(A_c) \frac{t_f}{N},$$

leading directly to the second result.

8.6 Proof for Theorem 30

PROOF.

Denote $(x(q), u(q), \sigma(q))$ the solution to Problem 9 generated by t_s^* and perturbed by q . For any $\epsilon > 0$, we

set $\eta = \min\{\epsilon L_l(t_f - t_s^*)/N, \frac{3\epsilon}{4}\}$. According to Theorem 28, there exists a t_s^* such that

$$\begin{aligned} v(t_s^*) &= m(x_{N+1}(0)) + \frac{t_f - t_s^*}{N} \sum_{i=1}^N l(\sigma_i(0)) \\ &\quad + t_s^* l(\rho_{\min}) \leq m^* + t_f l(\rho_{\min}) + \frac{\eta}{2} \end{aligned}$$

where m^* is the optimum of Problem 7 and $x_{N+1}(0)$ is the result of the unperturbed Problem 9 formed by t_s^* .

The first result follows from Theorem 21. The second result is from Theorem 20 as long as we choose δ sufficiently small such that $\|q\| \leq \delta$ is included in the cube area defined by Theorem 20. We now proceed to prove the third and fourth results.

According to Lemma 34,

$$m(x_{N+1}(q)) + \frac{t_f - t_s^*}{N} \sum_{i=1}^N l(\sigma_i(q)) + t_s^* l(\rho_{\min})$$

is a continuous function of q in a neighborhood of zero. Therefore, there exists a $\delta > 0$ such that for all $\|q\| \leq \delta$,

$$\begin{aligned} &m(x_{N+1}(q)) + \frac{t_f - t_s^*}{N} \sum_{i=1}^N l(\sigma_i(q)) \\ &\leq v(t_s^*) - t_s^* l(\rho_{\min}) + \frac{\eta}{2} \\ &\leq m^* + (t_f - t_s^*) l(\rho_{\min}) + \eta. \end{aligned}$$

Since $x_{N+1}(q)$ is feasible for the perturbed problem, we have $G(x_{N+1}(q)) = 0$ and $x_{N+1}(q)$ is feasible for Problem 7. Therefore, $m(x_{N+1}(q)) \geq m^*$ and

$$\frac{\sum_{i=1}^N l(\sigma_i(q))}{N} \leq \frac{\eta}{t_f - t_s^*} + l(\rho_{\min}).$$

As $\sigma_i(q) \geq \rho_{\min}$ for all i and l has positive derivative, we have

$$l(\rho_{\min}) \leq l(\sigma_i(q)) \leq l(\rho_{\min}) + \frac{N\eta}{t_f - t_s^*}.$$

Given that $\eta \leq \epsilon L_l(t_f - t_s^*)/N$ and the derivative of l is larger than L_l , we have

$$|\sigma(q) - \rho_{\min}| \leq \frac{N\eta}{L_l(t_f - t_s^*)} \leq \epsilon,$$

yielding the third result.

For the final result, since $l(\rho_{\min}) \leq l(\sigma_i(q))$, we have $m(x_{N+1}(q)) \leq m^* + \eta$. Furthermore, Theorem 21 indicates that

$$|m(\tilde{x}_{N+1}(q)) - m(x_{N+1}(q))| \leq NDL_AL_M\|B\|\|q\|,$$

where D , L_A , and L_M are defined in Theorem 21 and are constants when t_s^* is fixed. Thus, we obtain

$$m(\tilde{x}_{N+1}(q)) \leq m^* + \eta + NDL_AL_M\|B\|\|q\|.$$

With a sufficiently small $\|q\|$, we have $m(\tilde{x}_{N+1}(q)) \leq m^* + \epsilon$. \square

References

Behçet Açıkmese and Scott Ploen. A powered descent guidance algorithm for mars pinpoint landing. In

- AIAA Guidance, Navigation, and Control Conference and Exhibit*, page 6288, 2005.
- Behçet Açıkmeşe and Scott Ploen. Convex programming approach to powered descent guidance for mars landing. *Journal of Guidance, Control, and Dynamics*, 30(5):1353–1366, 2007.
- Behçet Açıkmeşe, Jordi Casoliva, John M Carson, and Lars Blackmore. G-fold: A real-time implementable fuel optimal large divert guidance algorithm for planetary pinpoint landing. *Concepts and Approaches for Mars Exploration*, 1679:4193, 2012.
- Behçet Açıkmeşe, M Aung, Jordi Casoliva, Swati Mohan, Andrew Johnson, Daniel Scharf, David Masten, Joel Scotkin, Aron Wolf, and Martin W Regehr. Flight testing of trajectories computed by G-FOLD: Fuel optimal large divert guidance algorithm for planetary landing. In *AAS/AIAA spaceflight mechanics meeting*, page 386, 2013.
- Behçet Açıkmeşe and Lars Blackmore. Lossless convexification of a class of optimal control problems with non-convex control constraints. *Automatica*, 47(2):341–347, 2011.
- HH Bauschke. Convex analysis and monotone operator theory in hilbert spaces, 2011.
- Dennis Bernstein. *Scalar, vector, and matrix mathematics: theory, facts, and formulas-revised and expanded edition*. Princeton university press, 2018.
- Jonathan Borwein and Adrian Lewis. *Convex Analysis*. Springer, 2006.
- Stephen P Boyd and Lieven Vandenberghe. *Convex optimization*. Cambridge university press, 2004.
- Michael D Canon, Clifton D Cullum Jr, and Elijah Polak. *Theory of optimal control and mathematical programming*. McGraw-Hill, 1970.
- John M Carson, Behçet Açıkmeşe, and Lars Blackmore. Lossless convexification of powered-descent guidance with non-convex thrust bound and pointing constraints. In *Proceedings of the 2011 American Control Conference*, pages 2651–2656. IEEE, 2011.
- Chi-Tsong Chen. *Linear system theory and design*. Saunders college publishing, 1984.
- Francis Clarke. *Functional analysis, calculus of variations and optimal control*, volume 264. Springer, 2013.
- Francis H Clarke, Yuri S Ledyaev, Ronald J Stern, and Peter R Wolenski. *Nonsmooth analysis and control theory*, volume 178. Springer Science & Business Media, 2008.
- Steven Diamond and Stephen Boyd. CVXPY: A Python-embedded modeling language for convex optimization. *Journal of Machine Learning Research*, 17(83):1–5, 2016.
- Kazuya Echigo, Christopher R. Hayner, Avi Mittal, Selahattin Burak Sarsilmaz, Matthew W. Harris, and Behçet Açıkmeşe. Linear programming approach to relative-orbit control with element-wise quantized control. *IEEE Control Systems Letters*, 7:3042–3047, 2023. doi: 10.1109/LCSYS.2023.3289472.
- Kazuya Echigo, Abhishek Cauligi, and Behçet Açıkmeşe. Expected time-optimal control: a particle model predictive control-based approach via sequential convex programming, 2024. Available at <https://arxiv.org/abs/2404.16269>.
- Purnanand Elango, Dayou Luo, Samet Uzun, Taewan Kim, and Behçet Açıkmeşe. Successive convexification for trajectory optimization with continuous-time constraint satisfaction. *arXiv preprint arXiv:2404.16826*, 2024.
- Matthew Fritz, Javier Doll, Kari C Ward, Gavin Mendeck, Ronald R Sostaric, Sam Pedrotty, Chris Kuhl, Behçet Açıkmeşe, Stefan R Bieniawski, Lloyd Strohl, et al. Post-flight performance analysis of navigation and advanced guidance algorithms on a terrestrial suborbital rocket flight. In *AIAA SCITECH 2022 Forum*, page 0765, 2022.
- Yaqi Guo, Qinyuan Liu, and Xiao He. Active fault diagnosis for stochastic systems subject to non-convex input constraints. *Automatica*, 164:111631, 2024.
- Matthew W. Harris. Optimal control on disconnected sets using extreme point relaxations and normality approximations. *IEEE Transactions on Automatic Control*, 66(12):6063–6070, 2021. doi: 10.1109/TAC.2021.3059682.
- Matthew W Harris and Behçet Açıkmeşe. Lossless convexification for a class of optimal control problems with linear state constraints. In *52nd IEEE Conference on Decision and Control*, pages 7113–7118. IEEE, 2013.
- Matthew W Harris and Behçet Açıkmeşe. Lossless convexification of non-convex optimal control problems for state constrained linear systems. *Automatica*, 50(9):2304–2311, 2014.
- Sheril Kunhippurayil, Matthew W Harris, and Olli Jansson. Lossless convexification of optimal control problems with annular control constraints. *Automatica*, 133:109848, 2021.
- Donggun Lee, Shankar A Deka, and Claire J Tomlin. Convexifying state-constrained optimal control problem. *IEEE Transactions on Automatic Control*, 68(9):5608–5615, 2022.
- Danylo Malyuta and Behçet Açıkmeşe. Lossless convexification of optimal control problems with semi-continuous inputs. *IFAC-PapersOnLine*, 53(2):6843–6850, 2020.
- Danylo Malyuta, Taylor P Reynolds, Michael Szmuk, Thomas Lew, Riccardo Bonalli, Marco Pavone, and Behçet Açıkmeşe. Convex optimization for trajectory generation: A tutorial on generating dynamically feasible trajectories reliably and efficiently. *IEEE Control Systems Magazine*, 42(5):40–113, 2022.
- Arkadi Nemirovski. Interior point polynomial time methods in convex programming. *Lecture notes*, 42(16):3215–3224, 2004.
- Sina Ober-Blöbaum, Oliver Junge, and Jerrold E Marsden. Discrete mechanics and optimal control: an analysis. *ESAIM: Control, Optimisation and Calculus of Variations*, 17(2):322–352, 2011.
- Suresh P. Sethi. *Optimal Control Theory: Applications to Management Science and Economics*. Springer Texts

- in Business and Economics. Springer, 4 edition, 2021. ISBN 978-3-030-91744-9.
- Joshua Shaffer, Chris Owens, Theresa Klein, Andrew D Horchler, Samuel C Buckner, Breanna J Johnson, John M Carson, and Behçet Açıkmeşe. Implementation and testing of convex optimization-based guidance for hazard detection and avoidance on a lunar lander. In *AIAA SciTech 2024 forum*, page 1584, 2024.
- Ronald Sostaric and Jeremy Rea. Powered descent guidance methods for the moon and mars. In *AIAA guidance, navigation, and control conference and exhibit*, page 6287, 2005.
- Nathaniel T Woodford and Matthew W Harris. Geometric properties of time-optimal controls with state constraints using strong observability. *IEEE transactions on automatic control*, 67(12):6881–6887, 2021.
- Runqiu Yang and Xinfu Liu. Convex hull relaxation of optimal control problems with general nonconvex control constraints. *IEEE Transactions on Automatic Control*, 69(6):4028–4034, 2023.
- Runqiu Yang, Xinfu Liu, and Defu Lin. Exact relaxation of nonconvex optimal control problems based on problem reconstruction. *Journal of Guidance, Control, and Dynamics*, 47(4):761–769, 2024.